NASA TECHNICAL MEMORANDUM

NATIONAL AERONAUTICS AND SPACE ADMINISTRATION U.S.A.

NASA TM X-3116

FABRICATION OF LIQUID-ROCKET THRUST CHAMBERS BY ELECTROFORMING

by Rudolph A. Duscha and John M. Kazaroff

Lewis Research Center

Cleveland, Ohio 44135

AMERICAN REVOLUTION BICENTENNIAL 1776-1976

1. Report No. NASA TM X-3116	2. Government Accession No.	3. Recipient's Catalog No.
4. Title and Subtitle FABRICATION OF LIQUID-ROCKET THRUST CHAMBERS BY ELECTROFORMING		5. Report Date November 1974
		6. Performing Organization Code
7. Author(s) Rudolph A. Duscha and John M. Kazaroff		8. Performing Organization Report No. E-7987
9. Performing Organization Name and Address Lewis Research Center National Aeronautics and Space Administration Cleveland, Ohio 44135		10. Work Unit No. 502-24
		11. Contract or Grant No.
12. Sponsoring Agency Name and Address National Aeronautics and Space Administration Washington, D.C. 20546		13. Type of Report and Period Covered Technical Memorandum
		14. Sponsoring Agency Code

15. Supplementary Notes

16. Abstract

Electroforming has proven to be an excellent fabrication method for building liquid rocket regeneratively cooled thrust chambers. NASA sponsored technology programs have investigated both common and advanced methods. Using common procedures, several cooled spool pieces and thrust chambers have been made and successfully tested. The designs were made possible through the versatility of the electroforming procedure, which is not limited to simple geometric shapes. An advanced method of electroforming was used to produce a wire-wrapped, composite, pressure-loaded electroformed structure, which greatly increased the strength of the structure while still retaining the advantages of electroforming. This report discusses the results of these programs with emphasis on practical aspects that have not been previously reported.

17. Key Words (Suggested by Author(s)) Electroforming Thrust chambers Forming techniques Electrodeposition Electroplating	18. Distribution Statement Unclassified – unlimited STAR category 34

19. Security Classif. (of this report) Unclassified	20. Security Classif. (of this page) Unclassified	21. No. of Pages 51	22. Price* $3.75

FABRICATION OF LIQUID-ROCKET THRUST CHAMBERS BY ELECTROFORMING

By Rudolph A. Duscha and John M. Kazaroff
Lewis Research Center

SUMMARY

Electroforming has proven to be an excellent fabrication method for building liquid-rocket, regeneratively-cooled thrust chambers. NASA sponsored technology programs have investigated both common and advanced methods. By using common procedures, several cooled spool pieces and thrust chambers have been made and successfully tested.

Thrust chambers have contained coating-protected tungsten liners, TD nickel liners, and graphite liners. Spool pieces have contained Hastelloy-X liners and coating-protected nickel liners. All of these designs were made possible by the versatility of the electroforming procedure, which is not limited to simple geometric shapes.

An advanced method of electroforming was used to produce a wire-wrapped, composite, pressure-loaded electroformed structure, which greatly increased the strength of the structure while still retaining the advantages of electroforming. Material strength improvement is also feasible by electrodepositing dispersion strengthened nickel. However, this procedure requires further development.

The process of electroforming is an established method of fabrication, However. for thrust chamber fabrication, problems such as variable material strengths, porosity, and bond separation can occur if the proper procedures are not carefully followed. This report discusses the various electroforming programs conducted by Lewis with emphasis on practical aspects that have not been previously reported.

INTRODUCTION

There are various methods for fabricating regeneratively cooled liquid-rocket thrust chambers; however, the best method for a particular design is not always obvious. The thrust chamber design, which basically consists of an inner wall, coolant passages, and an outer pressure shell, is based on specific heat transfer and stress calculations which may impose restrictions that will dictate the most suitable methods of fabrication. The material or materials selected, which must have the right combination of thermal conductivity,

strength, and other properties to produce a fully operable thrust chamber, may also restrict the available choices of fabrication methods. Other factors, such as dimensional accuracy, inspectability, combustion environment, and operating temperature and pressure, must also be considered in selecting the fabrication approach. For some applications one specific fabrication method may be the best or only choice. For other designs there may be several acceptable methods.

Most fabricated thrust chambers were made from brazed tube bundles of drawn, tapered, and formed tubes. The tube material was usually stainless steel. This fabrication technique is satisfactory for applications that typically have relatively low heat flux from the combustion gases to the hot-gas side wall. However, some of its disadvantages are high development costs, high cost for dimensional changes, if required, and difficulty in obtaining very small coolant flow areas in the throat region.

During the past few years, propellant combinations of interest to NASA have been flox-methane, hydrogen-oxygen, and hydrogen-fluorine. Each of these combinations affects the design and fabrication of thrust chambers in various ways. For example, the coolant passage design is very critical with the use of flox-methane propellants because methane is a relatively poor coolant and the heat fluxes are relatively high. Thus, the required coolant flow areas at the throat are extremely small for most operating conditions using flox-methane propellants. One of the most promising designs to accommodate these severe design conditions used rectangular channels and materials with high thermal conductivity, such as nickel. The use of nickel also provided the possibility of electroforming the thrust chambers through the buildup of thick sections using a plating bath.

To study electroforming and various advanced fabrication techniques, NASA sponsored a comprehensive technology program. These techniques were to be investigated primarily for application to the fabrication of thrust chambers, although the extension to injectors and other rocket engine components was also considered. This technology program consisted of several advanced fabrication contracts. The bonding techniques investigated were diffusion bonding, explosive bonding, brazing, and electroforming. Metal machining, forming, and joining techniques such as electric discharge machining, chemical etching, shear spinning, and electron beam welding were also investigated. The use of refractory metals, superalloys, and thermal barrier coatings were included in these programs. Small, subscale specimens and full-scale test hardware were built to evaluate the techniques. References 1 to 7 discuss in detail the individual contracted programs that were conducted under this overall technology program.

The electroforming process proved to be the most successful fabrication technique of those evaluated because of its versatility, reliability, and the cost of fabricated parts. Because of the success of this process, which is now being demonstrated by its use on the Space Shuttle main engine thrust chamber, this report was prepared to present a

comprehensive review of the state-of-the-art of electroforming as applied to liquid-rocket engine thrust-chamber fabrication.

The basic electroforming process will be described to provide a background for those unfamiliar with the process. Fundamental investigations related to the primary procedures for electroforming thrust chambers will be discussed. Finally, the actual electroforming of full-scale thrust chambers will be discussed. This report will concentrate on the experience gained and will discuss successes, failures, problems, and solutions. Also, recommendations to users of this process are provided with emphasis on the limitations and on potential problem areas that will require close control.

BASIC ELECTROFORMING PROCESS

The electroforming process is basically continuous electroplating on either a removable or nonremovable form. Electroplating is accomplished by means of electrolysis (fig. 1). The part to be electroformed is designated as the cathode. Metallic ions are transferred to the cathode through the electrolyte or bath. The anode consists of the material to be deposited on the cathode. Although not shown in the diagram, a typical bath also has to be constantly filtered to remove contaminants. The filtered solution is directed back into the bath to provide adequate agitation of the solution on the cathode's deposition surface. Movement of the cathode by revolution is also generally used to improve surface deposition. The electrolyte or bath consists of fused salts or solutions of various kinds. In commercial practice, the electrolyte is almost invariably an aqueous solution.

For the electroforming work discussed within this report, nickel is the only metal that was electroformed because (1) a considerable amount of experience existed for the commercial electroforming of nickel and (2) nickel properties provide for a design that is compatible with the heat-transfer requirements of the thrust chambers. Nickel may be electrodeposited from a wide variety of electrolytes, some of which are described in table I.

The nickel sulfamate bath is the primary bath used for electroforming thrust chambers. Boric acid, used for pH control, is added to the bath initially and periodically thereafter to maintain pH within the narrow range essential to producing deposits of uniform quality and mechanical properties. Chloride, in the form of nickel chloride, is used to insure proper anode solution to maintain the bath's proper nickel metal content over a large range of plating rates. Sulfur depolarized anodes are used as the nickel source. The agitation and revolving of the cathode are used to minimize hydrogen pitting, which can happen when evolved hydrogen bubbles adhere to the surface of the workpiece.

The properties of as-deposited nickel can vary considerably, depending on the plating conditions and the bath compositions. Table II shows mechanical properties obtained under

typical plating conditions for the various electrolytes listed in table I. In general, the nickel sulfamate electroforming solution used for thrust chambers results in deposits of low internal stress, high mechanical strength without loss of ductility, and good thermal stability and corrosion resistance.

It is not the intent of this report to elaborate on either the details of electroplating or the general process of electroforming. Excellent discussions on these subjects can be found in references 8 to 10.

FUNDAMENTAL INVESTIGATIONS OF
ELECTROFORMING AND BONDING

Typical thrust chamber electroforming normally proceeds from the inner structure (the hot gas side) to the outer structure. The inner structure could be electroformed nickel or another material depending on the specific application.

If the structure is to be made entirely of electroformed nickel, an inner mandrel is required. The outside of this mandrel must be machined to the required internal dimensions of the thrust chamber. This mandrel requires a parting medium so that it is easily removable after the electroforming is completed.

Two different procedures have been used successfully for the fabrication of thrust chamber cooling passages.

In the first procedure nickel is deposited onto the mandrel until a thickness is obtained that is equal to the hot-gas-side-wall thickness plus slightly more than the coolant passage height. A machining operation is required to produce the exact passage heights required along the length of the thrust chamber. Then the coolant passages are machined into the nickel. Finally, the outer structural jacket is electroformed over the coolant passages which have been filled with a soluble or low-melting-point filler material. This material must be easily removable and must be conductive or rendered conductive to permit electrodeposition to take place over the filler material. Each electroformer has his own process, and most of these are considered to be proprietary. One company has divulged its process in detail (ref. 4). Basically, a silver coating is applied to the passage filler material, which forms the conductive base for nickel to deposit onto, and the entire outer jacket is then electroformed. Proper cleaning and activation of the rib surfaces is a critical step needed to assure a strong bond. This can be done by anodically cleansing the surfaces in a sulphuric acid solution. Any contamination on this surface can prevent the formation of a high-strength bond. This could cause weak points in the bond and could be the ultimate cause for a bond failure. Typically, after electroforming of the outer structure is complete, a final machining is required to smooth or clean the outside surface. The filler material is removed by melting it

and flushing the workpiece with a solvent. Manifolds for the coolant are then installed at each end to complete the thrust chamber.

In the second procedure to fabricate cooling passages, nickel is deposited to a thickness slightly more than the hot-gas-side-wall thickness. A machining operation is required to produce the exact hot-gas-side-wall thickness. Then a machinable nonconductive substance is applied to the nickel to a thickness greater than the passage heights required. This covering is machined to produce a uniform surface that has a thickness slightly greater than the passage heights. Passages are machined in this covering down to and slightly into the first nickel layer. These grooves have the required width of the ribs that separate the coolant passages. The ribs are then "grown" by electroforming within these passages. A machining operation is then required to produce the forming exact coolant passage heights. At this point, the machinable nonconductive material remaining is removed, and the passages are filled with a soluble or low-melting-point material as described for the previous procedure. The remaining steps are the same as the previous procedure.

During the fundamental study of reference 5, this "grown-rib" fabrication procedure was investigated. The machinable nonconductive substance that was used was a vinyl. The part was dip-coated with liquid vinyl until a sufficient thickness was obtained. The vinyl was then cured and machined to a uniformly oversize thickness. The slots for the ribs were machined into the vinyl, and the nickel then electrodeposited into them. After a final machining process which cleaned off the tops of the ribs and left them the proper height, the vinyl was stripped out and the passages were filled with wax and rendered conductive by a proprietary process. The outer shell was then electroformed onto this ribbed structure.

Figure 2 shows a successful structure that passed the proof pressure test after the outer shell was electrodeposited. This indicated that both bonds were adequate. Figure 3 shows the results of an inadequate bond between the grown ribs and the inner shell. These bonds were torn loose during the machining of the tops of the ribs. An investigation determined that the reason for the bond failure was poor cleaning and inadequate activation of the inner wall surface before electroforming the ribs. Metallographic samples taken from the failure regions showed nickel sulfate crystals in the bond. There were areas where the as-machined surface was still visible, which indicates a nonbond condition. Other areas revealed material pulled out from the liner, which indicates a strong bond.

Severe thrust chamber operating conditions that produce high heat fluxes may require a material other than nickel for the inner hot-gas-side wall. Typically, the material could be Hastelloy-X, Inconel 718, Thoria dispersed (TD) nickel, or a similar, high-strength, high-temperature material. The conditions might even require an

5

inner coating such as zirconia applied to the hot-gas-side structural material. Coolant passages would be machined into the outside surface of this high strength material. and the thrust chamber then completed by electroforming as described.

Critical factors associated with the previously discussed fabrication methods are as follows:

(1) All of the electroformed bonds are critical and must be sufficiently strong to contain the internal coolant pressure. This includes the nickel rib to nickel inner-wall bond as well as the rib (either nickel or high strength material) to outer-wall bond.

(2) The filler material, which is used in the coolant passages before electroforming the outer jacket, must be easily and totally removable after the outer jacket has been electroformed.

(3) The electrodeposited nickel must have the required strength, and this strength must be reproducible from deposition to deposition.

(4) For the "grown-rib" approach, the machinable nonconductive substance must be readily machinable, dimensionally stable, and easily and totally removable.

These critical factors were investigated in detail during the program described in reference 6. Some additional key points of that program are reviewed here.

To obtain a strong bond between a deposited metal and any substrate, activation procedures must be used. These generally consist of mechanical, chemical, and electrochemical cleaning cycles. These are all dependent on the chemical composition of the substrate and the nature of the deposited metal. Reference 5 describes the procedures used for bonding electroformed nickel to Inconel 718, Hastelloy-X, and TD nickel.

For the bonding study reported in reference 5, a test specimen as shown in figure 4 was used to determine bond strengths. The substrate of the specimen was machined. A nickel disk was electrodeposited into the Lucite shield, thus providing a bond area at the end of the 0.635 centimeter (0.250 in.) diameter portion of the substrate. This specimen with the bonded disk was then placed in a split ring fixture. A tensile load was applied until the electrodeposited disk was pulled away from the substrate. Bond strengths were then calculated based on the bonded area and the failure load. Results for the three materials are shown in table III. Results of this investigation indicated the most difficult bonds to achieve were those of nickel to TD nickel.

In addition to the work on developing nickel-to-nickel and nickel-to-other-metal bonds, work during the program of reference 6 was also performed on developing nickel-to-plasma-sprayed-coating bonds. The use of low thermal conductivity, high operating temperature coatings on the inside of a thrust chamber provides a significant reduction in heat flux. This then reduces the operating temperature of the metallic structure of the thrust chamber.

6

The nickel-to-coating study involved coating the internal mandrel first and then electrodepositing the nickel on the coating. When the mandrel is finally removed, the remaining structure has an internal coating of low thermal conductivity, which serves as the required thermal barrier.

The coating materials used in the investigation were zirconia and alumina, the most widely used thermal barrier materials. These coatings are not conductive. Therefore, a method of rendering the coating surface conductive was developed so that the nickel could be electrodeposited onto the coating. The use of both electroless nickel and plasma sprayed nickel was investigated. Each material was applied to specimens of the coatings and were equally effective in producing a good nickel-to-coating bond while producing a pore-free surface for subsequent electrodeposition.

A procedure for mandrel removal had to be developed that did not disturb the coating. The procedure selected was to use an undersized stainless-steel mandrel, electrodeposit nonadherent copper onto it to the required dimensions, plasma spray the coating, plasma spray an initial conductive nickel layer, and then electrodeposit the subsequent nickel layer. When this was completed, the mandrel was withdrawn, and the copper was removed by dissolving it in nitric acid.

This procedure was evaluated by plasma spraying zirconia onto a copper tube, plasma spraying nickel over the zirconia, and then electrodepositing the next nickel layer. The copper was removed with nitric acid, and the remaining zirconia layer was examined by a qualitative spectrographic analysis. The copper content was determined as being less than one part in 10 000.

Two test cylinders were then made with coolant channels within them. One had a zirconia internal coating and the other had a graded zirconia internal coating. The graded zirconia consisted of 100 percent zirconia backed by three layers of mixtures of zirconia and Nichrome. These mixtures were 10 percent Nichrome-90 percent zirconia, 30 percent Nichrome-70 percent zirconia, and 70 percent Nichrome-30 percent zirconia. The procedure described was used for making these cylinders. Each cylinder was pressurized to evaluate bond integrity. There were no failures of the coating system due to internal pressure only. This fabrication procedure was then used to make the full-scale hardware described in the next section.

An important aspect of the overall fabrication process is that before producing an electroformed structure, tensile test specimens should be made in the same bath to be used for the desired electroformed structure. Electroforming was the major process used to produce two thrust chambers under contracts that were part of the overall technology program (refs. 4 and 6). These chambers are discussed more fully in the next section. However, preliminary electroformed nickel strength investigations were made for each of these chambers and will be discussed here.

The companies that did the electroforming provided the specimens from their respec
tive electroforming baths. These specimens were tested at Lewis both at room tempera-
ture and in liquid hydrogen. Liquid hydrogen was the coolant for these thrust chambers,
and there was no known data available for the tensile properties of electroformed nickel
at liquid-hydrogen temperatures before these tests. Figure 5 shows the design of the test
specimen. The thicknesses varied from 0.051 to 0.102 centimeter (0.020 to 0.040 in.) for
the various specimens. Figure 6 shows the reference 6 specimens after testing and fig-
ure 7 shows the reference 4 specimens. The clamping holes of two of the 0.051-centimete
(0.020-in.) thick specimens (fig. 6) elongated during tensile tests. To prevent this from
occurring for the thin specimens shown in figure 7, doubler plates were spot welded to the
pinned sections.

Table IV shows the results of these tests. As shown by the table, the reference 6
material was somewhat stronger than that of reference 4 but less ductile. For both mate-
rials strength and ductility were higher at liquid-hydrogen temperature. The results also
show the deviations in property values than can occur from bath to bath as well as from
day to day for the same bath. All of the baths were nickel sulfamate baths. These mate-
rial properties were more than adequate for the two separate thrust chamber designs that
the material was being used for. Details of these designs are presented in references 11
and 12.

FULL-SCALE TEST HARDWARE

The previous section discussed the preliminary investigations of test specimens and
sample parts that were made by the various electroforming companies. This section dis-
cusses the fabrication of five different full-scale hardware items to be used for actual hot
firing tests.

All of these items used electroforming as a key fabrication procedure. Two cooled
spool pieces (cylindrical sections of a thrust chamber) were made to put into practice the
results of the preliminary investigation of reference 5. Two different advanced design
concepts for regeneratively cooled thrust chambers with the same operating conditions
were made and used electroforming in two different ways. Finally, the knowledge acquired
during all of these efforts was applied toward fabricating a completely successful graphite-
lined thrust chamber.

Spool Piece Fabrication and Testing

The program of reference 5 showed that good bonds were obtained between
Hastelloy-X and electroformed nickel. Also, the results indicated that it was possible to
reliably bond electroformed nickel to a ceramic coating material such as zirconia.

Therefore, spool pieces with coolant passages and manifolds were designed based on these satisfactory results.

The first spool piece was made from a Hastelloy-X cylinder that had both the ribs of the coolant channels and the outer jacket electroformed onto it. This produced a structure that had an integral rib and coolant passage configuration. Figure 8 shows the details of this spool piece. The coolant manifolds with the necessary plumbing were attached by welding.

The second spool piece was a completely electroformed-nickel, cooled structure with the inner wall coated with the graded zirconia system described previously. This spool piece was made entirely from the inside out. First, a hardened steel mandrel was made. A nonadherent coating of electrodeposited copper was applied. The graded zirconia was plasma sprayed onto the copper. The electroformed nickel structure with machined coolant passages was made as described in the previous section. The electroformed nickel structure was removed from the steel mandrel. The copper was then removed by dissolving it in nitric acid. This left a cooled, electroformed nickel spool piece with an inner wall of plasma sprayed zirconia coating (fig. 9).

Each of these spool pieces was test fired at Lewis using hydrogen-oxygen propellants. Test runs were made at chamber pressures of 2.07 and 3.45 meganewtons per square meter (300 and 500 psia) over an oxidizer-fuel ratio (O/F) range of 4.5 to 6.0. Figure 10 shows the test results in terms of heat flux as a function of O/F. The test data represents several 5-second runs at each pressure for each chamber. There was also one 10-second run at 3.45 meganewtons per square meter (500 psia) for each chamber. Total testing included at least six separate firings for each chamber. For the highest chamber pressure the zirconia coating system decreased the heat flux to the thrust chamber by 50 percent for a nominal operating O/F of 5.8.

Figures 11 and 12 show the Hastelloy-X and the zirconia coated nickel spool pieces after firing. There was no discernible damage to either structure. The most significant result for the coated chamber is the excellent condition of the coating. For this type of coating application the spraying of the coating followed by the buildup of the electroformed structure is the recommended procedure. The problems associated with accessibility to small internal diameters when trying to plasma spray coatings into a thrust chamber as the last operation are thereby eliminated.

During the time of the reference 5 program, two other advanced fabrication programs were in progress (refs. 4 and 6). Each involved the use of electroforming as one phase of the process for the fabrication of complete thrust chambers. Both programs used the technique of construction that proceeded from the inside out.

Tungsten-Lined Thrust Chamber Fabrication and Testing

The first program of this type, described in detail in references 6 and 11, had the objective of producing an advanced thrust chamber design for use with hydrogen-fluorine propellants. One way of reducing the high heat fluxes that occur with these propellants is to use a plasma-sprayed thermal barrier on the hot-gas-side of the thrust chamber. However, the low-thermal-conductivity, thermal-barrier materials, such as alumina and zirconia, are not compatible with the fluorinated combustion gases.

Tungsten is a compatible, high-temperature material with a relatively high thermal conductivity. Therefore, the final design used both materials, tungsten and a plasma-sprayed zirconia. Tungsten was used as the hot-gas-side liner to protect the zirconia. The zirconia was used as the thermal barrier to provide a temperature drop that would produce a low back-side temperature. To provide thermal expansion compatibility, the zirconia was applied in graded layers in a mixture of zirconia and tungsten. The advantages of electroforming for making the nickel cooling jacket over this type of inner liner could be fully utilized for this thrust chamber design.

Fabrication proceeded from the inside out, starting with a disposable graphite mandrel. A tungsten-mesh-reinforced, vapor-deposited tungsten inner wall was created first on this mandrel. The graded zirconia and tungsten coating was plasma sprayed over this tungsten. The outer layer of this coating was then rendered conductive by plasma spraying a layer of pure nickel over it. Then an integral rib-coolant-channel-outer-jacket was made from electroformed nickel by the electroforming vendor as described in the previous section and reference 5. Manifolds of 304L stainless steel were welded on to complete the thrust chamber as shown in figure 13.

Several important aspects of the electroforming of this chamber are discussed in the following paragraphs. The outer nickel shell was 0.152 centimeter (0.060 in.) thick, which was sufficient for structural purposes. However, greater nickel thicknesses were required in the regions of the manifolds and the exit flange to provide sufficient material for welding. Because this was to be a test chamber and instrumentation was required, excess nickel up to 0.635 centimeter (0.250 in.) thick was electrodeposited as circumferential bands at the instrumentation locations. This provided sufficient thickness for machining of threaded holes into which thermocouples and pressure taps could be mounted. Figure 14 shows the chamber after machining and before welding.

Figure 15 is a photomicrograph of the cross section of a typical instrumentation hole extending into the coolant channel. Figure 16 shows more clearly the nickel layers produced by the various starts and stops that occurred during the electroforming of this total thickness.

While machining the exit flange after welding, an error was made and too much material was machined away at the closed ends of the coolant passages. The only practical

10

way to repair this was to electroform a sufficient thickness of nickel on to this region to contain the pressurized coolant. This electroformed repair was done satisfactorily. Figure 17 is a cross section of this region showing the various materials in this region. The 304L stainless-steel exit flange was electron beam welded on. A first attempt to correct the machining error was to gas tungsten arc weld a 304L stainless-steel ring on the end. Weld beads were laid at the inner diameter of this ring. However, this produced cracks in the thinned layer of electroformed nickel at the end of the channels. The final repair procedure was the deposition of nickel over this ring, completely enclosing the end.

While making this repair, leaks from the coolant channels to the inside wall were discovered in the exit nozzle. The tungsten and graded coatings were machined away to uncover these leaks in the original electroformed nickel. The leaks were small pores that extended from the inner surface of the nickel to the coolant channels. These pores obviously were formed as the nickel electrodeposition of the inner wall progressed outward.

An additional layer of electroformed nickel was then deposited in this region to seal the leaks. Figure 18 shows the extent of this repair. Several leaks still existed farther up the nozzle but were not significant enough to repair. This method of repair was possible because the region where electrodeposited nickel replaced the tungsten-coating layer was designed to operate with low enough heat fluxes that nickel alone would operate successfully. If nickel replaced the tungsten coating layer too near the throat, the temperatures would be too severe for the unprotected nickel.

This thrust chamber was tested at Lewis using hydrogen-fluorine propellants. At design operating conditions, a mixture ratio of 12, and a chamber pressure of 2.75 meganewtons per square meter (400 psia), the chamber produced 35 584 newtons (8000 lbf) of thrust. The initial test was run at a less severe heat flux condition produced by a mixture ratio of 8 and a chamber pressure of 2.07 meganewtons per square meter (300 psia). The test was run for a total of 4.0 seconds without any indication of a problem. Examination after shutdown revealed that the tungsten had overheated, although recorded nickel temperatures did not exceed 350 K (630° R). Figures 19 to 21 are photographs of the chamber after the test. Figure 19 is a view of the cylindrical combustion chamber taken from the injector end. The tungsten inner wall is blistered in several large areas. Figure 20 is a closeup of the blistered tungsten surface. Metallographic examination with the tungsten removed indicated that the graded coating underneath overheated also.

The overall cause for the failure can only be attributed to a lower thermal conductivity of the actual coating layer than that value that was used in the design. The best data available for the coating material were used; however, coating study programs that

were conducted after the chamber was tested revealed that considerable inconsistency can exist in the thermal conductivity of plasma sprayed coatings, up to a factor of two. If the actual value were half the design value, the temperature difference across the coating would be doubled. The predicted temperatures were 2475 K (4000° F) on the hot gas side and 700 K (800° F) on the nickel side. Therefore, the coating temperature could have been increased to over 3590 K (6000° F). This would raise the temperature of the tungsten also to well over 3590 K (6000° F) and cause the subsequent melting of both the coating and the tungsten.

Metallographic examination of the nickel indicated that there was no damage to the nickel. Figure 21 shows the exit region of the thrust chamber. All the tungsten and coating from the throat to the electroform repair section was completely removed during the test run. Examination showed that there was poor adhesion of the nickel to the coating. Apparently, on startup of the engine, the coating and tungsten were thermally shocked off.

There was no positive way to determine the actual cause of this poor adhesion. Any reason offered would only be speculation. The electroforming vendor did report that the plasma sprayed nickel surface was dirty and very difficult to clean before surface activation.

The entire electroformed nickel structure was undamaged. This included the original nickel as well as the nickel that was added to repair the chamber. In theory, the design of this thrust chamber, with the tungsten liner and graded zirconia coating between the nickel wall and the hot gas, provided a method for reducing the high heat fluxes associated with hydrogen-fluorine thrust chambers. However, because of the variability of the coating's thermal conductivity and the location of the coating between another high-temperature material and the cooled structure, the design proved to be unworkable. If the zirconia coating itself were exposed to a hot gas with which it is chemically compatible, the outer surface would melt or erode until thermal equilibrium is established.

The spool piece of reference 5 that had the zirconia adjacent to the hot gas proved the feasibility of this method for operation in a hydrogen-oxygen environment. The reliability of the nickel structure for both the spool piece and tungsten-lined thrust chamber shows that electroforming is a satisfactory technique for building thrust chambers.

Some problems do exist for the integral electroformed or "grown" rib technique. In the preliminary work discussed in the previous section, it was noted that the final machining tore these electroformed ribs loose. To produce these ribs, a removable substance has to be used into which grooves are machined; the grooves are then filled with electroformed nickel to create the ribs. For future work using this technique, it is recommended that further development be done to find a better removable material. However, it should be machinable without deforming so that accurate coolant passage dimensions can be maintained. It should also be easily removed after the ribs are electrodeposited.

12

For the tungsten-lined chamber the pass and a half cooling system with bifurcated passages required intricate machining. In some instances there was enough springback in the vinyl filler material during machining to slightly distort the rib configuration. There was also tooling chatter that left rough sides. This pattern was reproduced in the sides of the ribs and ultimately caused a pressure drop in the coolant passages that was greater than designed for.

Another problem associated with "growing ribs" is the limitation on the depth-to-width ratio that can be satisfactorily electroformed. Reference 6 discusses this problem, which occurred during fabrication of the tungsten-lined chamber. The limitation in depth-to-width ratio was thought to be in the range from 1 to 3. However, the lack of complete filling of the ribs in reference 6 occurred primarily in regions where the depth-to-width ratio was only 0.8. The location of the deposition problem was in the cylindrical portion of the chamber. This was considered to be the region where a problem was least likely to occur. This result provides further evidence that the technique of growing coolant passage ribs requires more development.

Figure 22 shows a cross section of the ribs as they were electrodeposited in the cylindrical portion of the chamber. The rib growth did not occur uniformly, as generally assumed. Figure 23 is an enlargement of the upper part of one rib, showing the area that did not completely fill in during the original deposition. The top edges of this void were ground back by hand, leaving a wider opening to facilitate deposition into the void. The subsequent closeout electroforming filled in this depression very well as shown by figure 23.

Thoria-Dispersed Nickel-Lined Thrust Chamber Fabrication

This thrust chamber was also to be used with hydrogen-fluorine propellants and had the same operating conditions as the tungsten-lined chamber. However, a different design approach was used. The inner liner material was TD nickel, a superalloy that is compatible with fluorine and has good high-temperature strength and high thermal conductivity. The inner liner was made from two sections of spun TD-nickel welded together. Total thickness of the liner was equal to the hot-gas-side wall thickness plus the coolant passage height. Figure 24 illustrates the design concept.

Coolant passages were machined into the TD nickel liner by electrical discharge machining. This method was chosen so that both the width and height of the coolant passage could be tailored to produce the lowest possible material temperatures while maintaining minimum coolant pressure drop.

Electroforming was used in two stages for fabrication of the thrust chamber under this program: to build up material at both ends of the liner before machining the coolant channels and to build the outer jacket after the passages were machined.

Thick material at each end of the liner was required for adequate welding of the inlet and exit manifolds and the attachment flanges. This built-up material was required before channels were machined because this material also formed the inlet and exit of each channel. Figure 25 shows the nodular growth that occurs at edges during relatively thick electrodepositing. The center portion of the chamber has been masked off, and deposition takes place only at the ends. Periodic machining of such nodules is necessary to restart uniform nickel deposition.

Special techniques and equipment were required to produce the necessary preferential deposition of nickel at the liner ends. This was accomplished by using auxiliary anodes, shields, masking, thief rings, and bipolar anodes. Figure 26 shows the installation of special equipment on the thrust chamber, and figures 27 and 28 show schematically various arrangements required to produce the desired amount of material.

Figures 29 and 30 are photomicrographs that show the various layers that were required to complete the buildup previously described. Figure 29 shows the complete section of the coolant inlet manifold region. The end flange and the manifold with the diverter plate were welded on by the gas tungsten arc process. Figure 30 is an enlarged view of figure 29 showing the electrodeposited nickel layers in more detail. The photomicrographs show several voids, which apparently did not affect the welding operation, but did provide a source of cracking during operation.

During the plating of the outer shell, two problems occurred that are common to relatively thick deposits. While deposition takes place hydrogen is evolved as a consequence of the process. This hydrogen formation results in hydrogen bubbles forming on the surface. If these bubbles are not removed, they will cause a porous structure to be formed. During the first 0.51 to 1.02 millimeters (20 to 40 mils) of outer jacket deposition, many pores of about 0.51 to 0.76 millimeter (20 to 30 mils) diameter were discovered in the nickel in several regions. Even though agitation of the fluid onto the surface was being used, it was not effective in removing all of the hydrogen bubbles.

In this process the bubble is not merely trapped by the deposited nickel but slowly moves out with the surface buildup, thereby forming discrete continuous holes in the structure. To correct this, the material that contained these holes was machined away, and the deposition process was restarted with improved agitation. Figure 31 shows the arrangement of the spray agitation that proved to be effective in eliminating the pores in the nickel.

As with the tungsten-lined chamber, excess outer jacket thickness was required to provide machined instrumentation assembly holes. An extra 0.508-centimeter (0.200-in.) thickness made a total required thickness of 0.914 centimeter (0.360 in.). When depositing thicknesses this large, the inherent nodular growth of the electroforming process becomes severe. This requires intermediate steps of machining to keep the surface from becoming porous due to the nodules. Figure 32 shows the surface after the electroforming was

complete and before a final machining. Figure 33 shows the completed thrust chamber after finish machining, and manifold and flange installations.

The other problem encountered during fabrication of the chamber was attainment of a strong bond between the TD nickel and electroformed nickel over the entire surface of the chamber. During the proof pressure test of the TD nickel chamber, two bond failures occurred about 170° apart in the exit nozzle at 4.14 meganewtons per square meter (600 psi). (See figs. 34 and 35.)

Metallographic examination of these bulges indicated that they were caused by separation at the bond line due to trace amounts of thorium oxide on the rib surface. Figure 36 is a cross section of the second bulge showing the separation at the bond line. Figure 37(a) is an enlargement of the first good bond adjacent to the separation. The initial 0.076 millimeter (0.003 in.) electrodeposited nickel layer on the TD nickel rib can be seen followed by the next two layers. Figure 37(b) shows an enlarged view of the bond separation adjacent to the rib with the preceding good bond. The separation occurred between the TD nickel rib and the first thin nickel layer.

The source of this thorium oxide is the TD (thoria dispersed) nickel liner material. Activation of wrought TD nickel is more complicated than the activation of pure wrought nickel. The anodic acid cleaning of the TD nickel surface dissolves nickel and releases minute amounts of the thorium oxide that is dispersed within the metallic structure. This thorium oxide is resistant to most acid cleaning solutions. Mechanical scrubbing can remove all of the visible material; however, trace amounts are undetectable and result in small sites of nonbond.

Graphite-Lined Thrust Chamber Fabrication and Testing

The experience gained from the previous programs was applied in the fabrication of a graphite-lined regenerative thrust chamber designed for use with flox-methane propellants. One major objective of the chamber design was to reduce the high heat fluxes resulting from the use of these high performance fluorinated propellants. Another major objective was to produce a thrust chamber amenable to slight design changes without greatly affecting the cost of fabrication.

At that time considerable experience had been gained in the fabrication and testing of uncooled graphite thrust chambers, so that a cooled design with a graphite inner wall appeared feasible. Graphite and fibrous graphite materials had demonstrated the ability to withstand temperatures of 3035 K (5000° F) for short firings while being subjected to a fluorinated combustion environment.

For extended firings the graphite has to be cooled to keep its inner surface temperature at 3035 K (5000° F) or lower. To accomplish this, the regenerative jacket containing the coolant passages had to be in intimate contact with the graphite. The only method

available to fulfill that requirement was electroforming. Figure 38 shows the resulting thrust chamber design.

The graphite material selected was AG Carb-101, a fibrous graphite with excellent thermal shock resistance. The inner liner was made from four separate graphitized sections that were glued together. Figure 39 shows these sections before gluing. A mandrel was inserted into the center and the outside contour final machined. Figure 40 shows the graphite after machining. Nickel was then electroformed over the graphite and contour machined. Constant width coolant passages were mechanically milled into the nickel (fig. 41). This channelled structure was then closed out with a 0.254-centimeter (0.100-in.) thick layer of electrodeposited nickel. The manifolds were welded on, completing the thrust chamber (fig. 42). A thorough discussion of this program is presented in reference 7.

The thrust chamber was successfully test fired for a total of 525 seconds with 21 separate starts. Included in the test program was a cycle test of eight continuous cycles of 5 seconds on and 2 seconds off. The longest continuous run was 220 seconds. There was no damage or deterioration of the thrust chamber. The graphite liner remained intact with no measurable erosion. The nickel regenerative cooling jacket was structurally sound and performed as designed.

During the fabrication process, an electroform repair was required for both of the graphite-lined thrust chambers. As was the case with the TD nickel thrust chamber, the most difficult area to electroform was the exit end flange, which required excess material for manifold welding. Discrepancies occurred in the area of the exit end flange of both thrust chambers. During leak testing, leaks were found around the entire circumference of the flange approximately 3.18 millimeters (1/8 in.) inside of the manifold weld. The leaks were due to laminations in the nickel that were opened by the heat of welding. No indication of these laminations was evident during the dye penetrant inspection performed before welding.

Repairs for both thrust chambers were made by building up nickel on the face of the exit end flange. Figures 43 and 44 illustrate the repair procedures used.

Both completed thrust chambers were pressure tested at 13.1 meganewtons per square meter (1900 psi) with water. Dye penetrant inspection performed before the pressure tests showed no indication of cracks or porosity. However, 22 weeping type leaks were present on serial number 1 thrust chamber and two similar leaks were present on serial number 2 thrust chamber. These were pores that existed in the outer 0.254-centimeter (0.100-in.) thick shell. The leaks in serial number 1 thrust chamber were closed by spot gas-tungsten-arc welding on the outside surface. The leaks of serial number 2 thrust chamber were not significant and were not repaired. A pressure check of this chamber between tests indicated several more weeping type leaks existed. The

subsequent successful firing of this thrust chamber indicated that they were of small consequence.

This program was a good example of the use of electroforming to build a structure that could not easily be made any other way. The intimate contact over the entire graphite surface was a necessary requirement to assure uniform cooling of the graphite. During testing, the graphite hot-gas-side wall was consistently and uniformly kept in the range of 2755 K (4500° F).

In summary, two problems that are uniquely associated with electroforming occurred during the fabrication of the full-scale test hardware: (1) Areas that required excess material buildup proved to be critical and required the use of special techniques and equipment to combat nodule growth. The extra machining and restarts resulting from nodule formation require close control so that undesired (and possibly undetected) laminations do not occur. (2) The problem of porosity was again present, as evidenced by the detection of the weeping type leaks. Proper surface agitation with the plating solution can preclude the occurrence of these pores.

ADVANCED THRUST CHAMBER FABRICATION CONCEPTS

A technology program was conducted to investigate methods of increasing the strength of electroformed nickel. Increased strength is desirable to reduce the outer wall thickness and thereby reduce thrust chamber weight. Two means of increasing the strength of electroformed nickel structures were investigated: dispersion strengthening and wire wrapping.

Dispersion strengthened materials are normally made by the powder metallurgy process. Finely divided oxide particles, such as alumina or thoria, are mixed with powders of the basic metal, and the mixture is then compacted, sintered, and rolled to achieve the desired metallurgical structure. The advantage of this dispersed-phase structure is that the oxide particles key the structure to make it stable, especially at high temperatures.

Therefore, the advantage of an electroformed dispersion strengthened nickel would be its improved high-temperature strength and resistance to recrystallization and creep at high temperatures. In addition, dispersion strengthened electroforming would allow complicated items to be made that would be extremely difficult to make with dispersion strengthened materials produced by the conventional powder metallurgy process.

Wire-reinforced electroformed nickel would have yield strength properties comparable with those of high-nickel-content alloys. This could be accomplished by wrapping fine, specially shaped, high-strength wire around a liner and then electrodepositing nickel between and over the wires. This procedure could be repeated in layers until the required thickness is obtained.

17

In this program (see ref. 45), cylindrical burst-test specimens of various materials were made and tested. Strength comparisons were made between standard nickel cylinders made from a nickel sulfamate bath, dispersion strengthened cylinders, and wire wrapped cylinders. The standard cylinders had an average hoop tensile strength of 551.6 meganewtons per square meter (80 000 psi). The dispersion strengthened cylinder's hoop tensile strength was 689.5 meganewtons per square meter (100 000 psi). The wire reinforced cylinders averaged about 861.9 meganewtons per square meter (125 000 psi) in hoop tensile strength.

The void formation between wires that had previously been a problem was eliminated through the use of D-shaped wires. These wires were wrapped with the flat side down (see figs. 45 and 46). Two wire sizes were used, 0.025 by 0.051 centimeter (0.010 by 0.020 in.) and 0.010 by 0.020 centimeter (0.004 by 0.008 in.). The wire was 302 stainless steel. The large wire had a tensile strength of 1875.4 meganewtons per square meter (272 000 psi), and the small wire had a tensile strength of 2689.4 meganewtons per square meter (390 000 psi).

Cylinder burst tests were made for the cylinders fabricated with the large wire. The wire in these cylinders occupied only 15 percent of the volume of the total cylindrical material. Cylinders with the stronger wire wrapped with a greater volume percent of wire would produce greater increases in strength over the standard nickel than was obtained during this program.

For the dispersion strengthening work, both alumina and thoria particles were used. Both materials produced dispersed nickel with inconsistent strengths: Test specimen strengths varied from less than to greater than the strength of standard nickel. The thoria dispersed nickel strength was more consistent than the alumina dispersed nickel and was, therefore, used to make the burst test cylinders for comparison.

Of the two strengthening methods, the wire wrapped method was clearly the better. The dispersion strengthening process, in addition to being inconsistent, is also complex and would require considerably more development. On the other hand, the wire wrapped strengthening method is readily feasible. Further development would be required, but the results of this program provided a logical procedure to follow.

Additional work is required to optimize wire size and spacing between wires. The process to wrap continuously on a cylinder while simultaneously plating should be developed to produce a multilayered, wire-reinforced structure. Finally, the results of both of these efforts should be applied to continuously wrap and plate using optimum wire size and spacing on the contoured surface of a thrust chamber.

CONCLUDING REMARKS

The primary purpose of these programs was to evaluate the various fabrication procedures investigated as applied to full-scale thrust chambers. Each process was verified through the use of small test specimens. Where there were difficulties, they occurred when fabrication of the full-scale article was attempted, which pointed up dramatically the necessity for fabricating full-scale hardware in order to properly evaluate the fabrication processes.

Results from the use of thermal barriers indicate that the most successful way to build coated electroformed chambers is to spray the coating on a mandrel and electroform onto the coating. This procedure eliminates any restrictions as to a minimum internal diameter that can be successfully coated. It also allows the coating process to proceed uninterrupted from one end to the other. Internal spraying usually requires two steps with overlapping in the throat region.

Variations in electrodeposited material properties can occur from bath-to-bath or even from day-to-day in the same bath. Because of this, test samples should be run along with each piece of hardware to verify the properties of the deposited material. Current densities can vary somewhat between the test sample and the part due to geometry differences, but even though this occurs, the test specimen will still indicate reasonably accurately the material properties of the part.

Porosity in electroformed material is another potential problem that requires attention. Porosity occurs for two reasons: (1) the conductivizing process used on nonconducting surfaces and (2) hydrogen bubble formation. In the conductivizing process any small area that is not made conductive results in the growth of pores. Extreme care must be exercised to insure the entire piece is conductivized. Hydrogen bubble formation can be eliminated by proper surface agitation to sweep these hydrogen bubbles away from the surface.

A buildup of large material thicknesses in specific locations, especially the ends, produces nodular growth. These nodules can lead to undetected laminations that could cause ultimate failure of the part. Machining of these nodules before extreme growth occurs can reduce the tendency toward lamination buildup. Increasing the number of starts and stops for a given buildup increases the chances for an improper surface condition and thus a poor bond. Extreme care should be taken in both designing and electroforming thick deposits.

The electroforming of a coolant jacket over a graphite liner illustrates the advantage of the electroforming process to provide intimate contact over complicated geometries. To produce a machined fit over such a complex surface that would guarantee 100 percent surface contact for heat-transfer purposes would be very difficult and costly.

Wire wrapped reinforced electroformed structures offer the advantage of the versatility of electroforming combined with the strength resulting from the use of high strength wire. This method has application to many pressure containment structures in addition to hardware investigated thus far.

SUMMARY OF RESULTS

Electroforming has been used successfully for the fabrication of liquid-rocket regenerative-cooled thrust chambers. NASA supported advanced technology programs have investigated a variety of thrust chamber designs using electroforming to improve fabrication procedures, reduce costs, produce lighter weight chambers, and provide greater flexibility for design changes. A summary of the direct results of these programs follows:

1. The basic nickel sulfamate bath produces electroformed nickel with properties that are completely adequate for many thrust chamber applications.

2. Strong bonds can be obtained between electroformed nickel and high strength materials such as Inconel 718 and Hastelloy-X. Good bonds between electroformed nickel and thoria dispersed nickel are more difficult to obtain.

3. Electroformed nickel can be bonded to plasma sprayed thermal barrier coating materials, such as zirconia. This allows a coated thrust chamber or similar type of structure to be made starting from the inner surface and working out.

4. The method of growing ribs by electroforming permits the use of a bifurcated passage design. However, the procedure requires development to obtain better machinable material for the formation of grooves for rib deposition. The deposition process requires knowledge of the actual limitations on depth-to-width ratios for the grooves.

5. Areas of thick material deposition must be carefully formed so as not to produce hard-to-detect laminations. If not detected and repaired, these laminations may cause failure of the part during proof testing or operation.

6. Material strength improvement through dispersion strengthening is feasible. However, the procedure requires more development to make it practical.

7. Strength improvement through wire wrapping to produce an electrodeposited-metal, high-strength wire composite structure is both feasible and practical.

Lewis Research Center,
National Aeronautics and Space Administration,
Cleveland, Ohio, July 23, 1974,
502-24.

REFERENCES

1. Ashurst, A. N.; Goldstein, M.; and Ryan, M. J.: Development of Advanced Fabrication Techniques for Regeneratively Cooled Thrust Chambers by the Gas-Pressure-Bonding Process. Battelle Memorial Institute (NASA CR-72795), 1970.

2. Smith, E. G., Jr.; Laber, D.; Linse, V. D.; and Ryan, M. J.: Development of Explosive Welding Techniques for Fabrication of Regeneratively Cooled Thrust Chambers for Large Rocket Engine Requirements. Battelle Memorial Institute (NASA CR-72878), 1971.

3. Milam, T. B.: Thermal Skin Fabrication Technology. PWA-FR-4976, Pratt & Whitney Aircraft (NASA CR-120988), 1972.

4. Dietrich, F. J.; and Leach, A. E.: Advanced Thrust Chamber Designs. BAC-8489-945001, Bell Aerospace Co. (NASA CR-72996), 1971.

5. Hammer, S.; and Czacka, Z.: Development of Advanced Fabrication Techniques for Regeneratively Cooled Thrust Chambers by the Electroforming Process. Camin Laboratories (NASA CR-72698), 1969.

6. Stubbs, V. R.: Investigation of Advanced Regenerative Thrust Chamber Designs. Aerojet-General Corp. (NASA CR-72742), 1970.

7. Stubbs, V. R.: A Graphite-Lined Regeneratively Cooled Thrust Chamber. Aerojet Liquid Rocket Co. (NASA CR-120853), 1972.

8. Symposium on Electroforming — Applications, Uses, and Properties of Electroformed Metals. ASTM STP 318, American Society for Testing and Materials, 1962.

9. Lowenbeim, Frederick A., ed.: Modern Electroplating. 2nd ed., John Wiley & Sons, 1963.

10. ASM Metals Handbook. Vol. 2 — Heat Treating, Cleaning and Finishing, 8th ed., American Society of Metals, 1964.

11. Stubbs, V. R.; Evensen, H. M.; Fraczek, E. W.; and Cunningham, J. A.: Investigation of Advanced Regenerative Thrust Chamber Designs. Aerojet-General Corp. (NASA CR-72266), 1967.

12. Brown, C. H.: Investigation of Advanced Thrust Chamber Designs. BAC-8489-945001, Bell Aerospace Co. (NASA CR-72320), 1968.

13. McCandless, Lee E.; and Davies, Larry G.: Development of Improved Electroforming Techniques. GTC-297, General Technologies Corp. (NASA CR-134480), 1973.

14. Nickel Plating Process and Properties. International Nickel Co., 1967.

15. Brenner, A.; and Jennings, C. W.: Physical Properties of Electrodeposited Metals. Plating, vol. 35, 1948, pp. 1228-1239.

TABLE I.- NICKEL ELECTROLYTES AND OPTIMUM CONCENTRATIONS

Electrolytes	Nickel sulfamate	Nickel sulfate	Nickel chloride	Nickel fluoborate	Boric acid	Other	Reference
	Optimum concentration, kg/m^3 (oz/gal)						
Sulfamate, electrotyping	412 (55)	0 (0)	11.2 (1.5)	0 (0)	37 (5)	- - - - - - - - - - - - - - - - - -	14
Sulfamate, conventional	449 (60)		7.5 (1.0)		37 (5)	- - - - - - - - - - - - - - - - - -	14
Sulfamate, concentrated	599 (80)		.5 (.7)		40.5 (5.4)	- - - - - - - - - - - - - - - - - -	14
Sulfamate, no chloride	449 (60)		0 (0)		30 (4)	- - - - - - - - - - - - - - - - - -	8
Sulfamate, hard	247 (33)		7.5 (1.0)		30 (4)	Stress reducer	14
All chloride	0 (0)		300 (40)		30 (4)	- - - - - - - - - - - - - - - - - -	8 and 14
High chloride		187 (25)	157 (21)		37 (5)	- - - - - - - - - - - - - - - - - -	14
Watts type, 1 normal Ni		105 (14)	30 (4)		30 (4)	- - - - - - - - - - - - - - - - - -	15
Watts type, 2 normal Ni		210 (28)	60 (8)			- - - - - - - - - - - - - - - - - -	15
Watts type, 3 normal Ni		300 (40)	60 (8)			- - - - - - - - - - - - - - - - - -	14
Watts type, 4 normal Ni		427 (57)	120 (16)			- - - - - - - - - - - - - - - - - -	15
Watts type, hard		262 (35)	45 (6)			Stress reducer	14
Hard nickel		255 (34)	0 (0)			Ammonium chloride, 24.7 (3.3)	8
Fluoborate		0 (0)	0 (0)	300 (40)		Fluoboric acid, 37 (5)	14

23

TABLE II.- TYPICAL MECHANICAL PROPERTIES FROM NICKEL ELECTROLYTE DEPOSITS

Electrolytes	Plating temperature		Acidity, pH	Current density		Tensile strength		Elongation in 5.08 cm (2 in.), percent	Reference
	K	°F		A/m^2	A/ft^2	MN/m^2	ksi		
Sulfamate, electrotyping	317	110	4.0	1293	120	482.6	70	16	14
Sulfamate, conventional	333	140	4.0	539	50	620.9	90	10	14
Sulfamate, concentrated	333	140	4.0	2155	200	482.6	70	14	14
Sulfamate, no chloride	331	135	4.5	431	40	786.0	114	11	8
Sulfamate, hard	328	130	5.0	646	60	896.0	130	6	14
All chloride			2.0	539	50	689.5	100	14	14
High chloride			3.0			517.1	75	20	14
Watts type, 1 normal Ni			3.0			448.2	65	18	15
Watts type, 2 normal Ni			3.0			386.1	56	28	
	304	86	1.5			724.0	105	11	
	328	130	5.6			696.4	101	5	
Watts type, 3 normal Ni	328	130	3.0			413.7	60	28	14
Watts type, 4 normal Ni	328	130	3.0			564.4	82	8	15
Watts type, hard	323	122	5.0			1172.2	170	2	14
Hard nickel	328	130	5.6	646	60	1048.0	152	5 to 8	8
Fluoborate	328	130	2.7	323	30	399.9	58	30	14

TABLE III.- BOND STRENGTH OF NICKEL ELECTRODEPOSITED

ONTO OTHER METALS

Material	Testing done at -			
	Room temperature		811 K (1000° F)	
	Bond strength			
	MN/m^3	ksi	MN/m^3	ksi
Inconel 718	710.3	103	310.3	45
Hastelloy-X	689.5	100	365.4	53
TD nickel	641.2	93	200.0	29

TABLE IV.- TENSILE TEST DATA OF ELECTROFORMED NICKEL

Test temperature	Sample	Ultimate tensile strength		0.2-percent yield strength		Elongation, percent
		MN/m^2	ksi	MN/m^2	ksi	
Specimens from ref. 6 material						
Liquid hydrogen	1	1144	166	641	93	17
	2	1081	157	565	82	(a)
	[b]3	- - -	- - -	- -	- - -	- -
Room	4	836	121.4	503	72.9	9
	5	800	116.0	499	72.4	11
	6	809	117.3	506	73.4	9
	7	806	117.0	488	70.8	8.5
Specimens from ref. 4 material; bath A						
Liquid hydrogen	1	806	117	372	54	17
	2	765	111	400	58	11
	[c]3	924	134	490	71	9
Specimens from ref. 4 material; bath B						
Room	1	474	68.8	255	37	20
	2	493	71.5	276	40	17
Liquid hydrogen	3	744	108	330	47.9	40
	4	731	106	323	46.9	37.5
Room	[d]5	455	66	276	40	23
	[d]6	455	66	276	40	23
	[d]7	482	70	289	42	22

[a]Total sample elongated.

[b]Specimen did not break; elongated holes.

[c]Specimen 3 material made on different day than specimens 1 and 2 material.

[d]Specimens 5 to 7 material made on a different day than mate-ial for specimens 1 to 4.
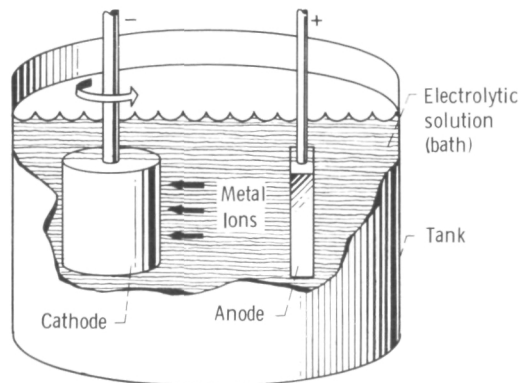
Figure 1. - Simplified electroforming setup.
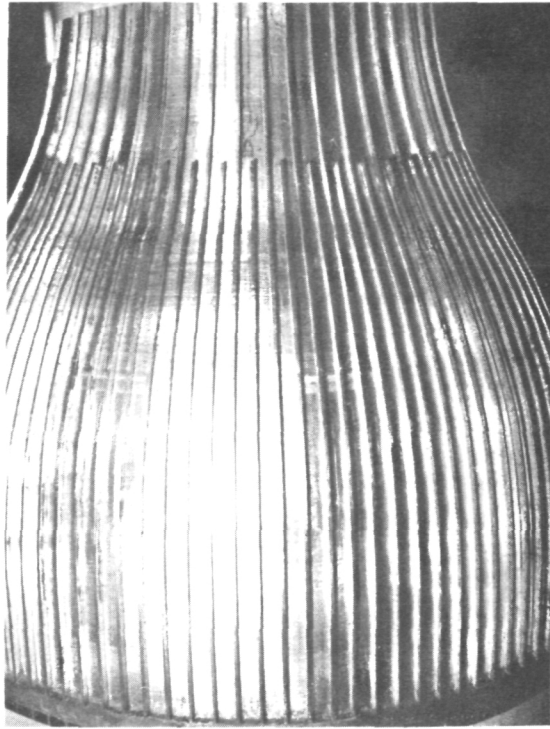
Figure 2. - Segment of thrust chamber showing electroformed integral rib structure with bifurcated coolant passages.

C-70-1585

Figure 3. - Grown-rib structure torn loose during machining.

Lucite
shield

0.635 cm
(0.250 in.)

Substrate

(a) Before deposition.

Split ring die

Electroformed nickel

Bond line

Table

Substrate

Load

(b) After deposition.
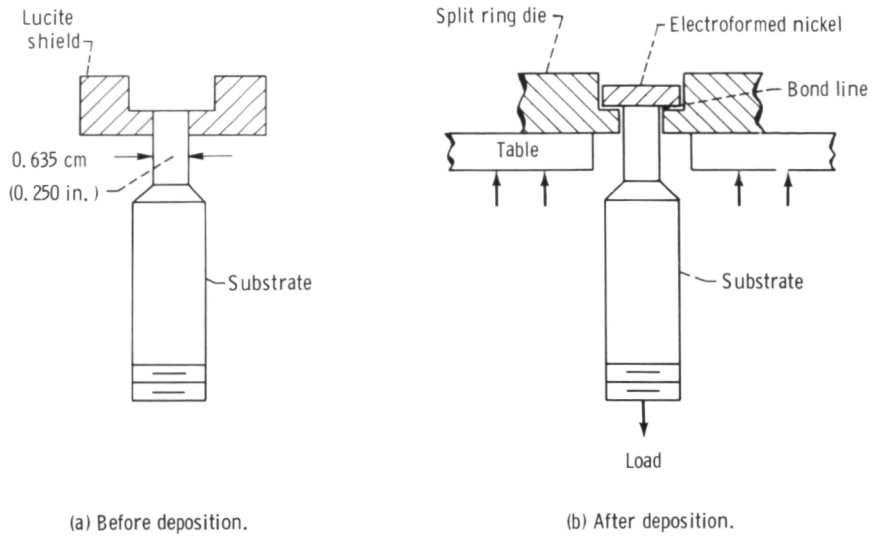
Figure 4. - Adhesion strength specimen.

20.32 cm (8 in.)

1.27 cm (0.500 in.)

5.08 cm (2 in.)
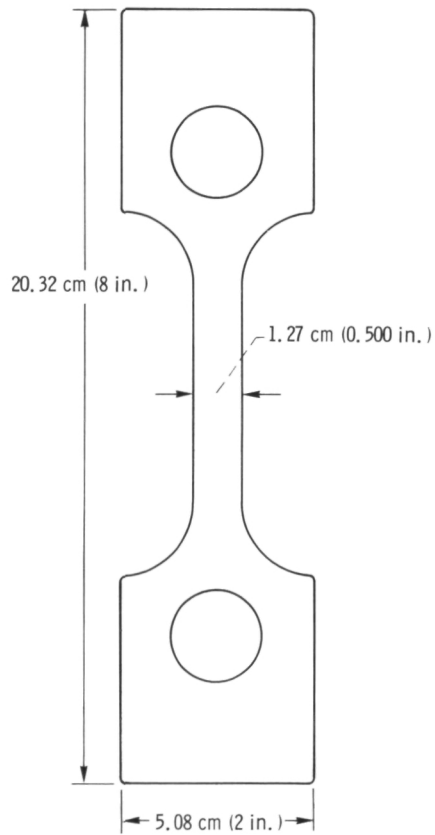
Figure 5. - Tensile specimen for electroformed nickel.
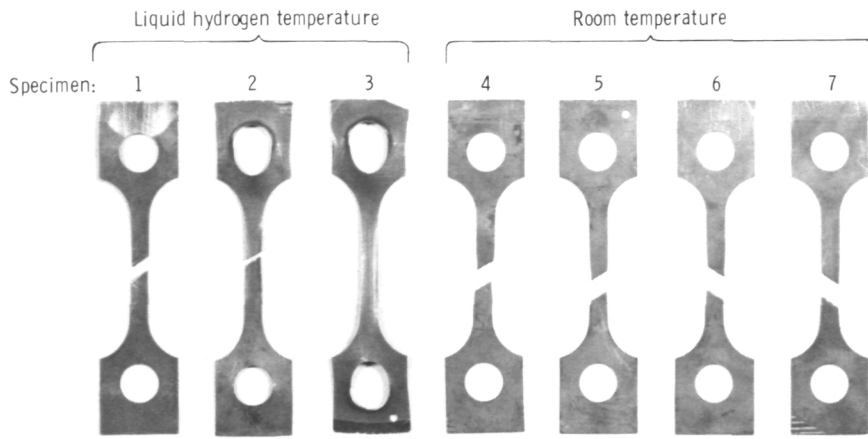
Figure 6. - Electroformed nickel tensile specimens after testing (ref. 6 material).
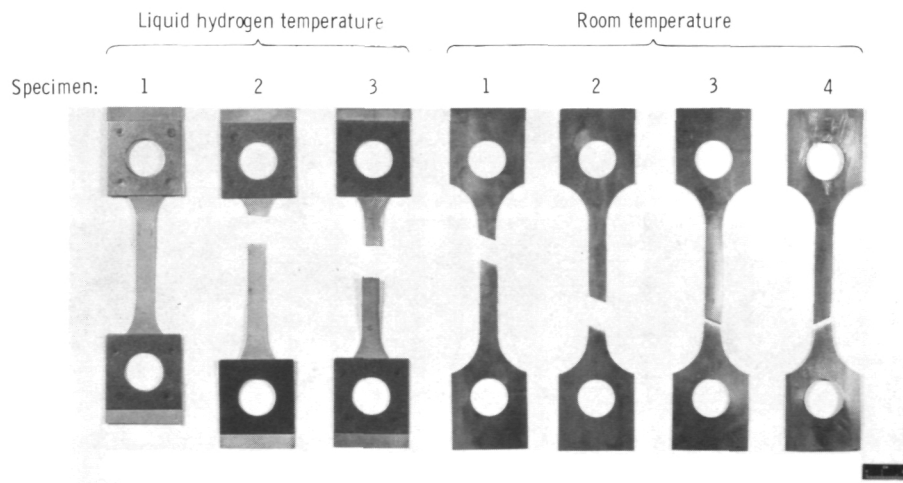
Figure 7. - Electroformed nickel tensile specimens after testing (ref. 4 material).
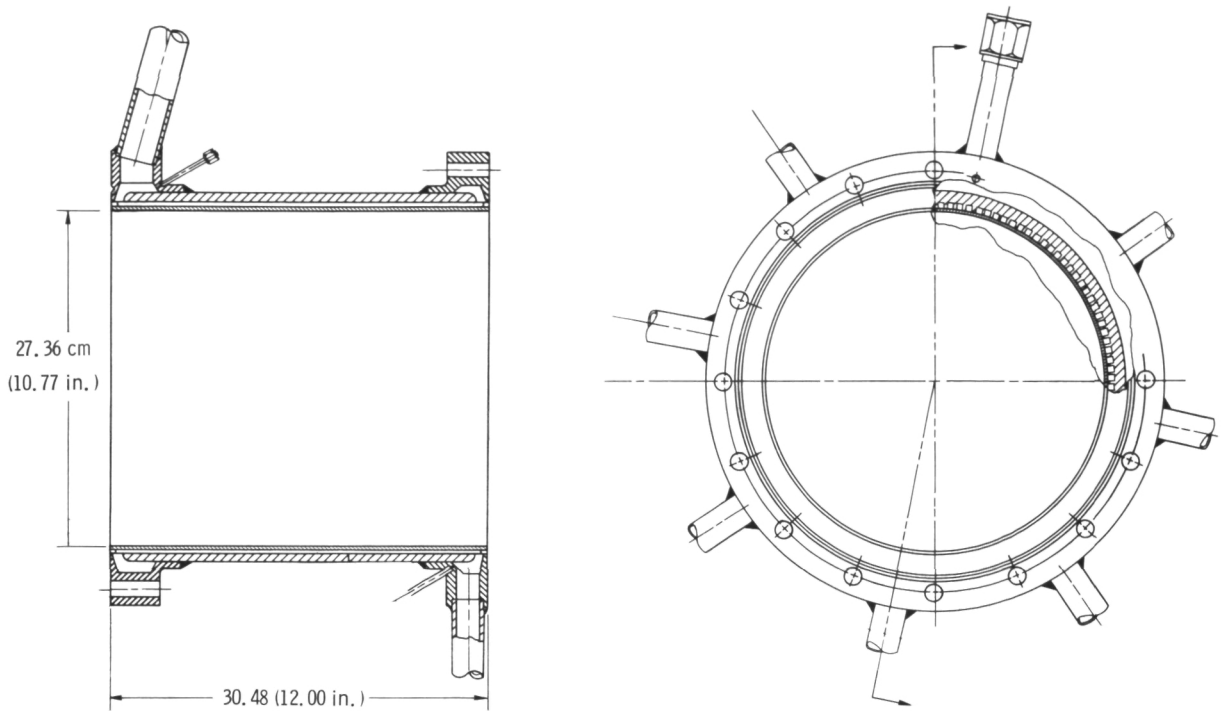
Figure 8. - Details of spool piece design.

C-69-1548
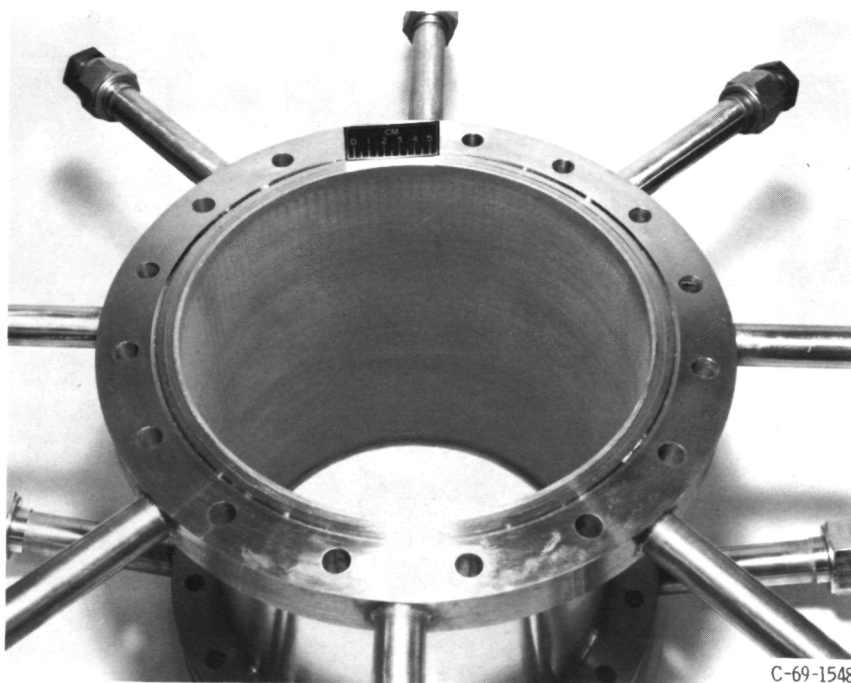
Figure 9. - Zirconia coated spool piece before firing.
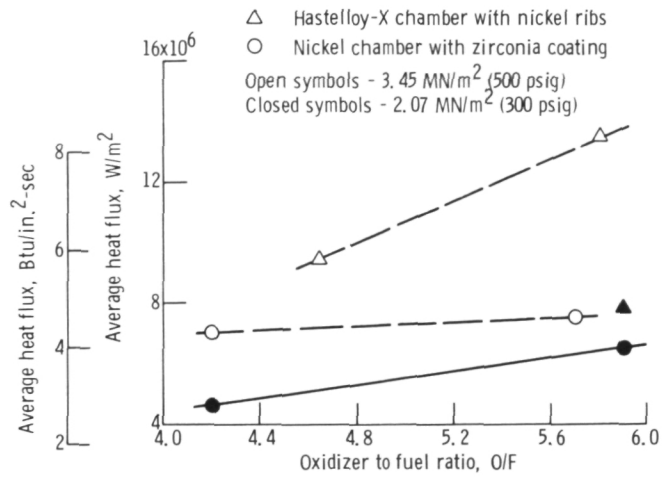
Figure 10. - Test results from water cooled thrust chamber tests.

C-69-3357
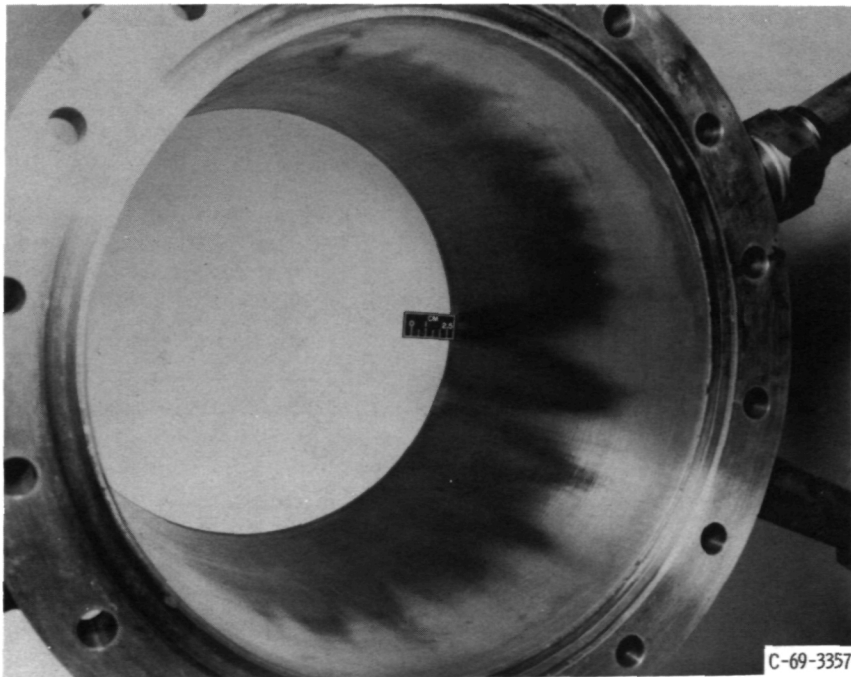
Figure 11. - Hastelloy-X spool piece after firing.

30
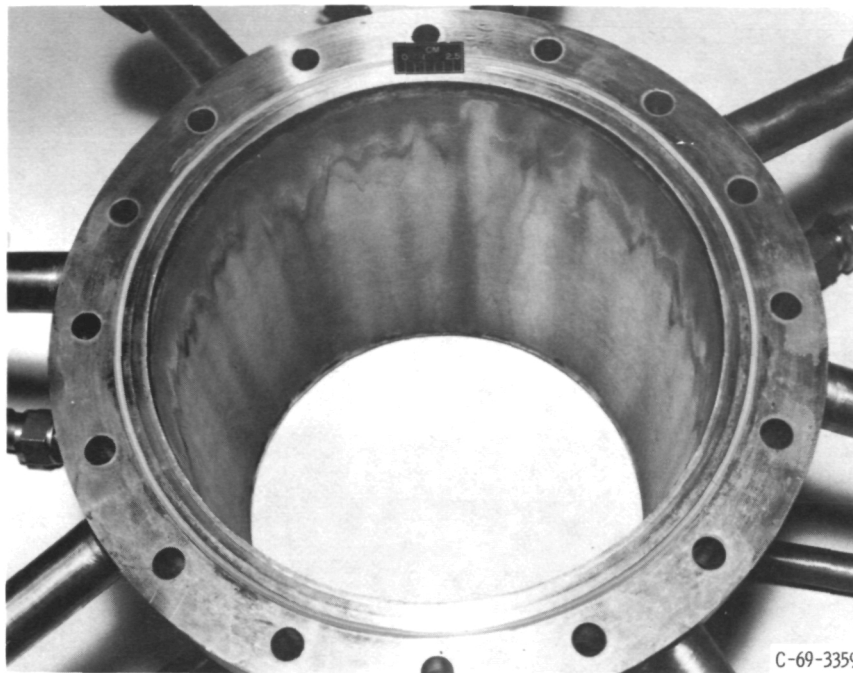
Figure 12. - Zirconia coated spool piece after firing.

Figure 13. - Tungsten-lined thrust chamber with plumbing attached.
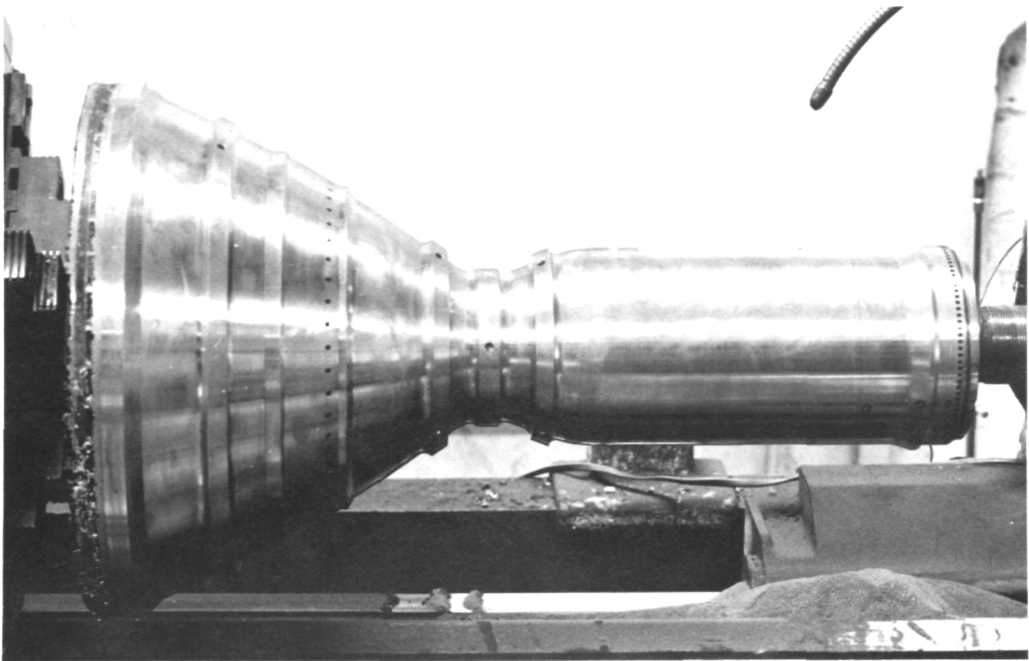
Figure 14. - Final machining of electroformed nickel outer jacket before welding on the manifolds and flanges.

Outer Jacket

Instrumentation hole

Coolant passage

Grown rib

Inner shell
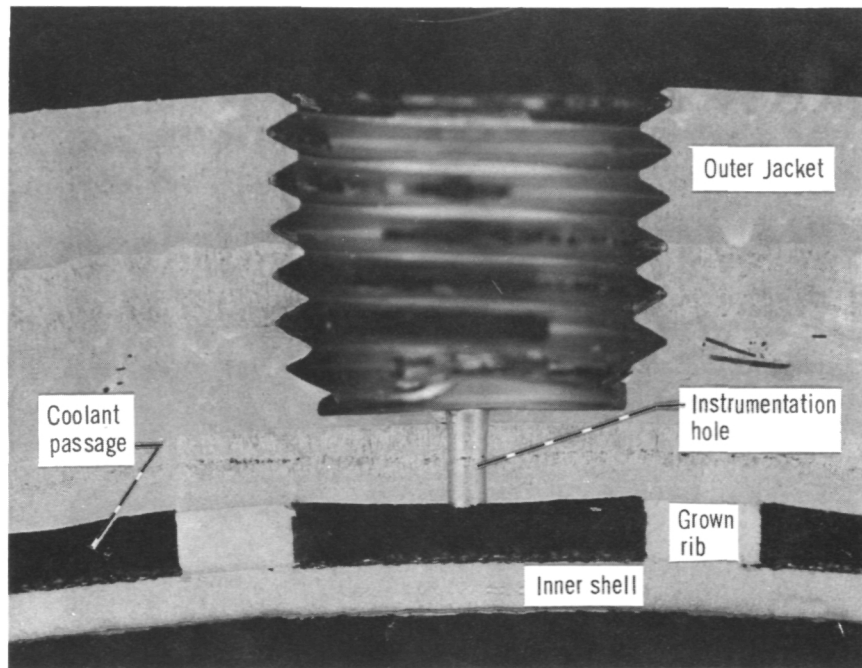
Figure 15. - Section taken through instrumentation hole.
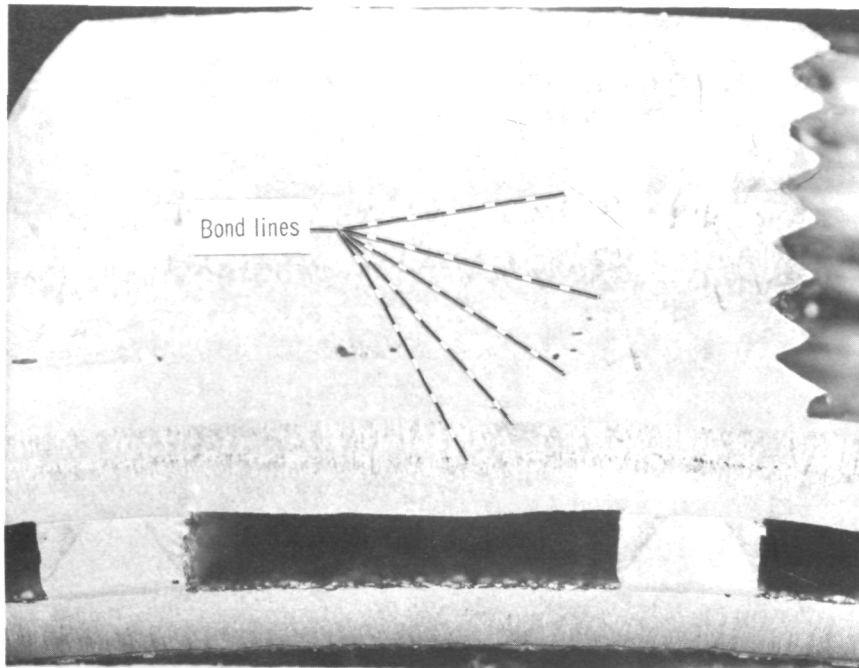
Figure 16. - Enlarged section showing electroformed nickel layers.
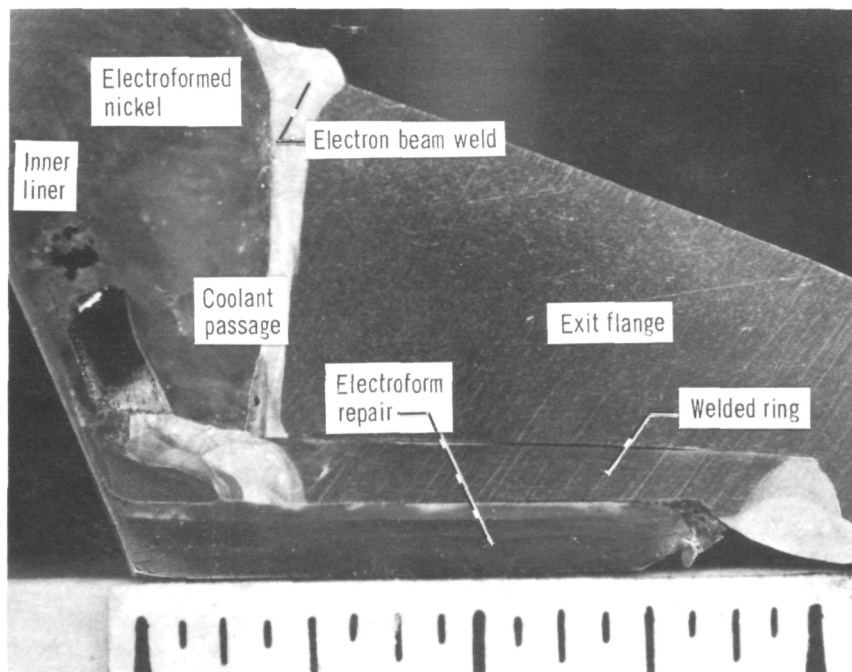
Figure 17. - Exit end showing repaired region.
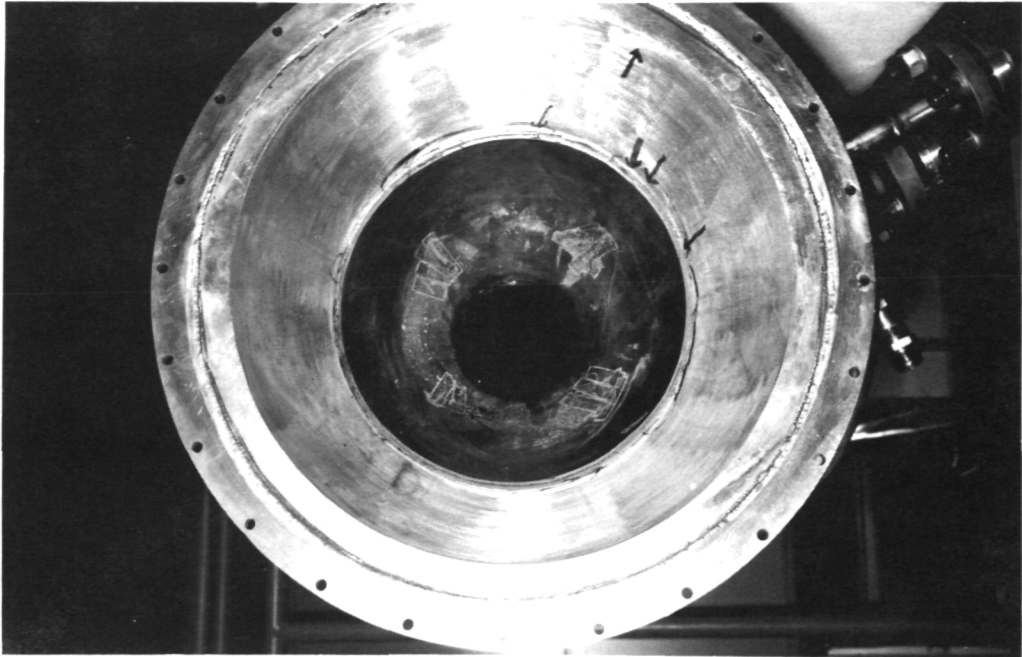
Figure 18. - Final electroform repair of aft end showing areas of leakage.
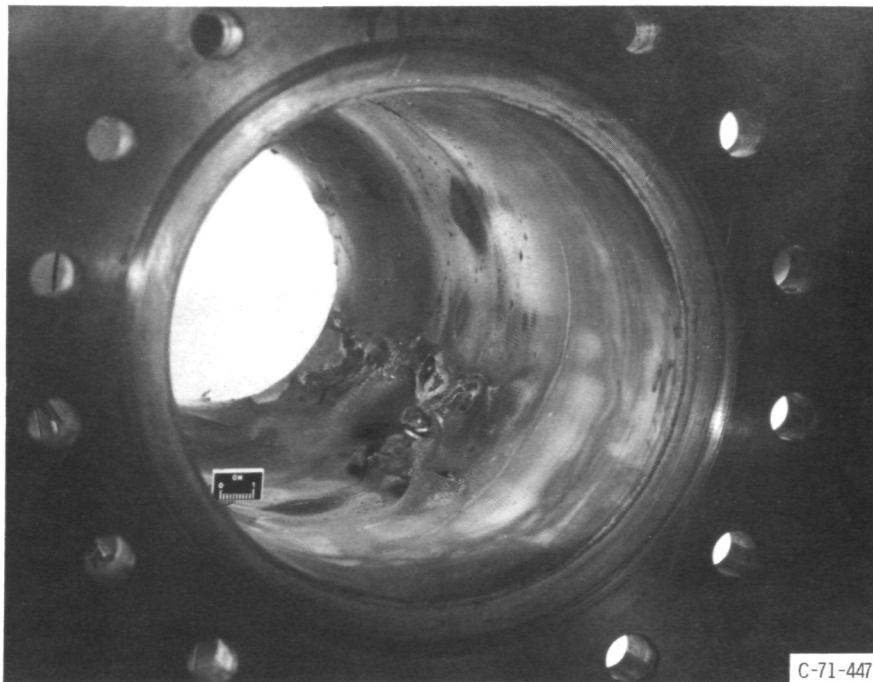
C-71-447

Figure 19. - Blistered tungsten surface viewed from injector end.
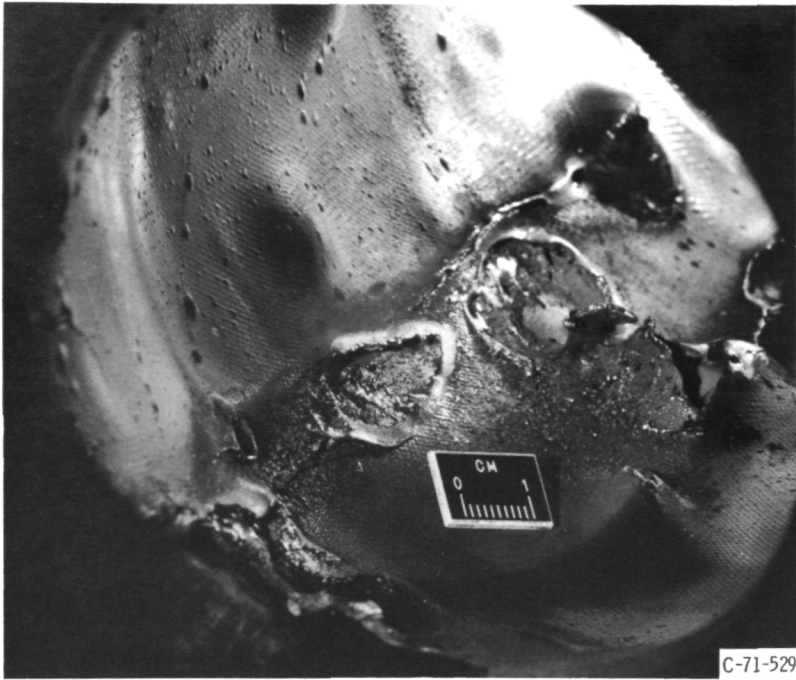
Figure 20. - Closeup of blistered tungsten surface.
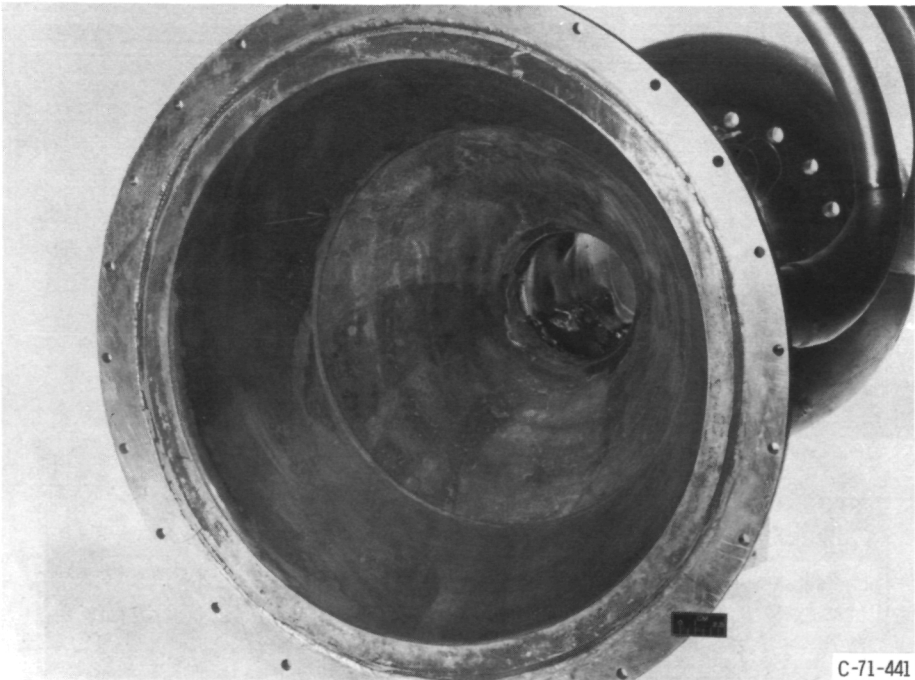
Figure 21. - Exit region showing bare nickel after loss of tungsten liner.
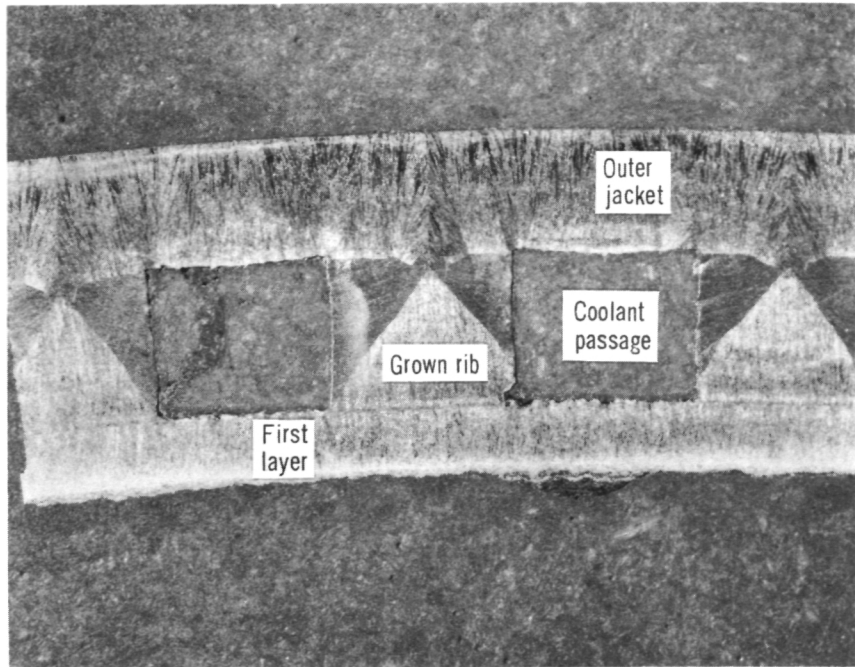
Figure 22. - Section showing grown-rib structure.
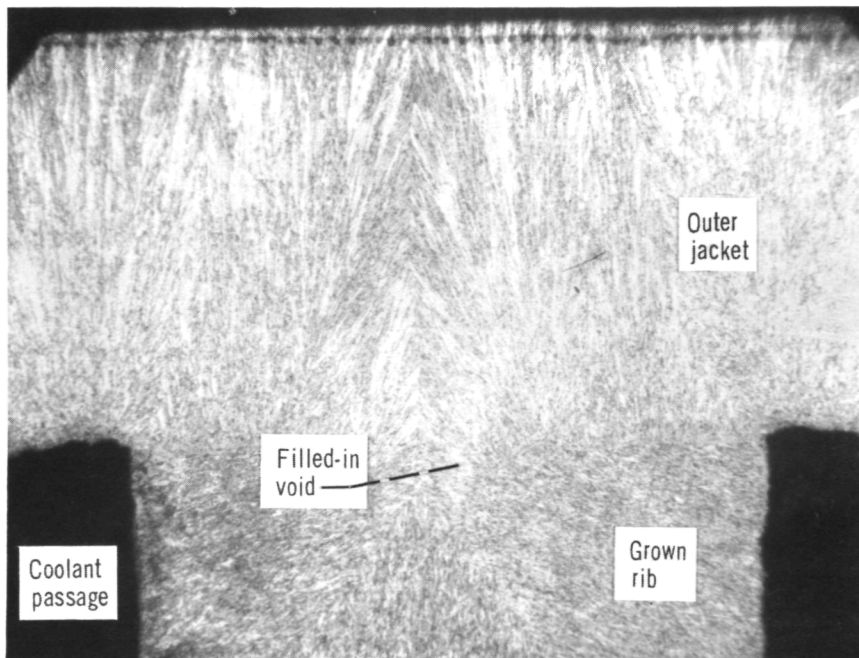
Figure 23. - Enlarged section of grown rib showing filled in depression.

Channel width:
  Aft, 0.650 cm (0.256 in.)
  Forward, 0.279 cm (0.110 in.)

Liner thickness:
  Aft, 0.239 cm (0.094 in.)
  Forward, 0.279 cm (0.110 in.)

Spun TD nickel
chamber liner

304 stainless
steel aft manifold

Channel depth:
  Aft, 0.163 cm (0.064 in.)
  Forward, 0.203 cm (0.080 in.)

Inner shell
(spun TD
nickel liner)

Electrodischarge
machined channels

Outer shell
(electroformed
nickel)

Electrodischarge
machined flow
channel

304 stainless steel
forward manifold

69.78 (27.48 in.)

12.05 cm (4.75 in.)
diam throat

53.98-cm (21.25-in.)
diam aft flange

0.408 cm (0.160 in.)
thick outer shell
(electroformed nickel)

22.9-cm (9-in.)
diam forward flange

0.915 cm (0.360 in.)
thick outer shell
(electroformed nickel)

0.408 cm (0.160 in.)
thick outer shell
(electroformed nickel)

Figure 24. - Advanced regeneratively cooled thrust chamber.

37

Figure 25. - Nodular growth during electroforming of flange ends.
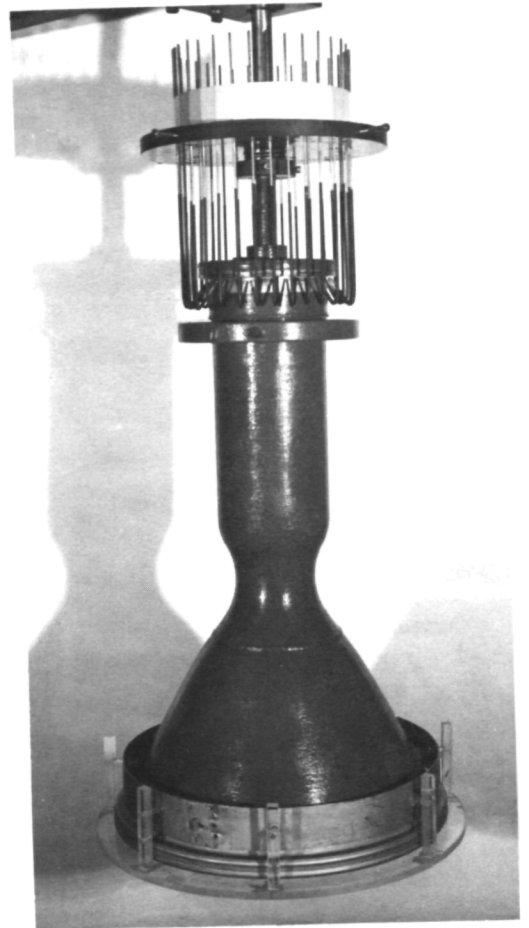
Figure 26. - Auxiliary anodes and shields for preferential electroform deposition.
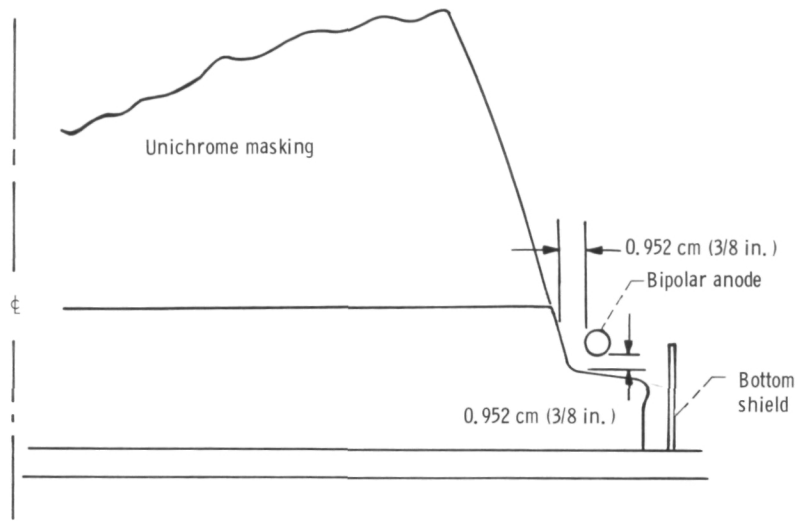
Figure 27. - Bipolar anode setup for preferential electroform deposition.

Labels in figure: Unichrome masking; 0.952 cm (3/8 in.); Bipolar anode; Bottom shield; 0.952 cm (3/8 in.)
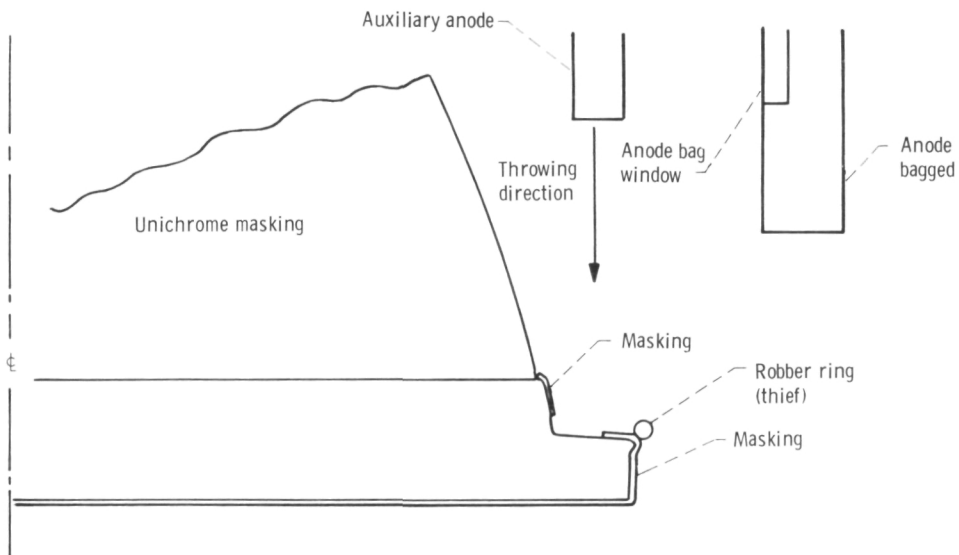
Figure 28. - Masking and thief ring setup for preferential electroform deposition.

Labels in figure: Auxiliary anode; Anode bag window; Anode bagged; Throwing direction; Unichrome masking; Masking; Robber ring (thief); Masking
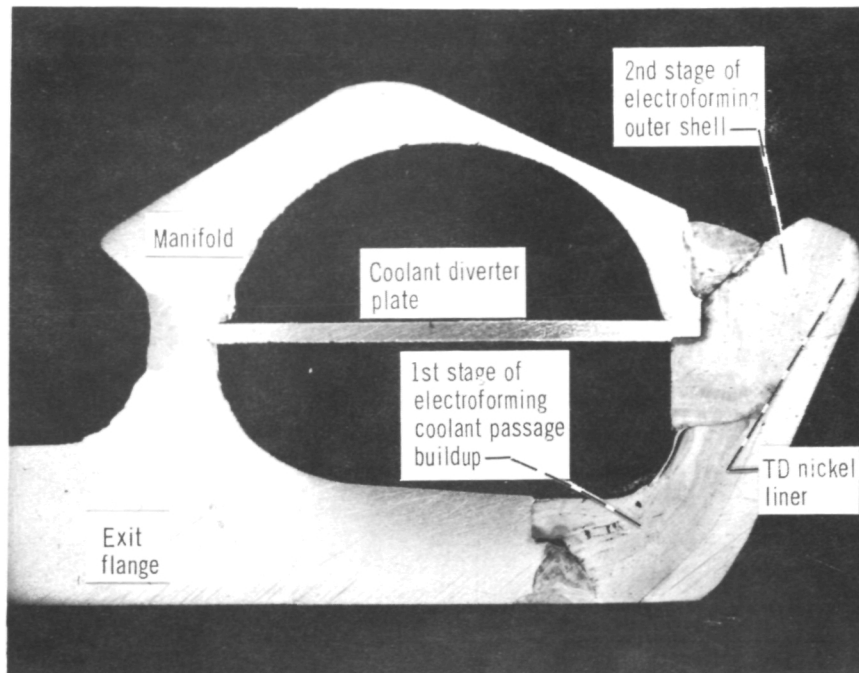
Figure 29. - Section of coolant inlet manifold region of TD nickel.
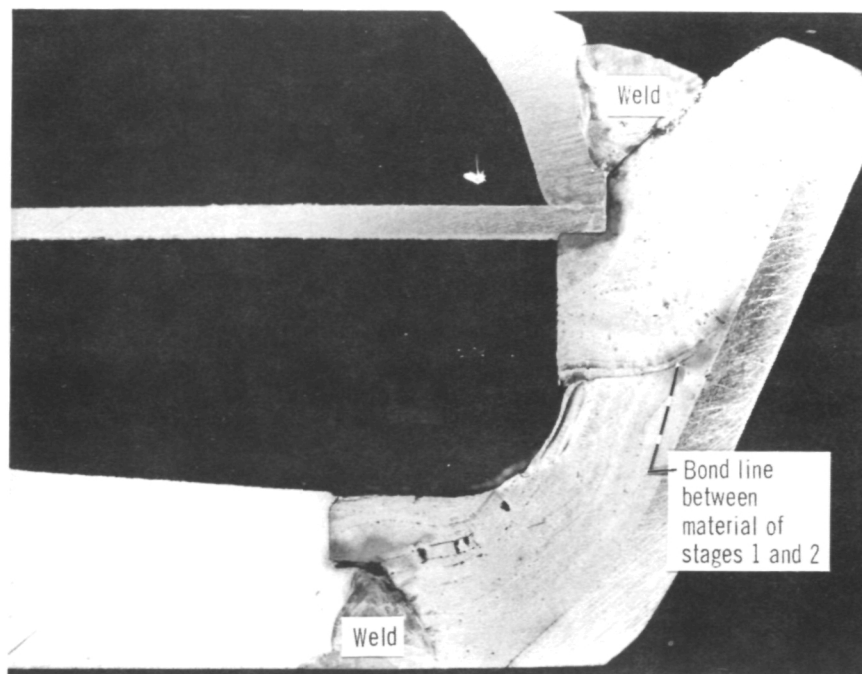
Figure 30. - Enlarged view of manifold section.
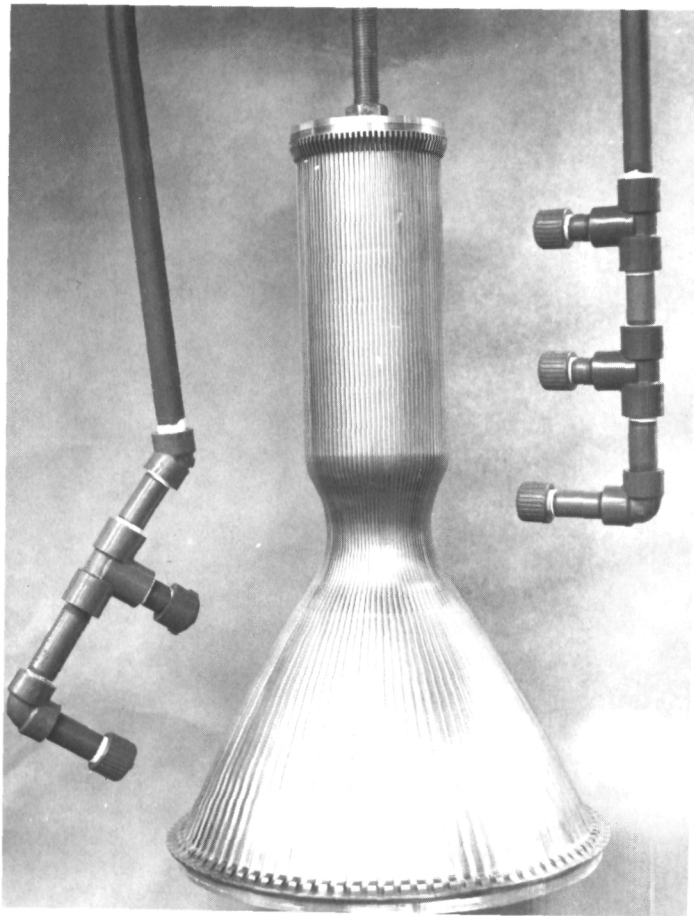
Figure 31. - Electrolyte spray agitation for electroforming.
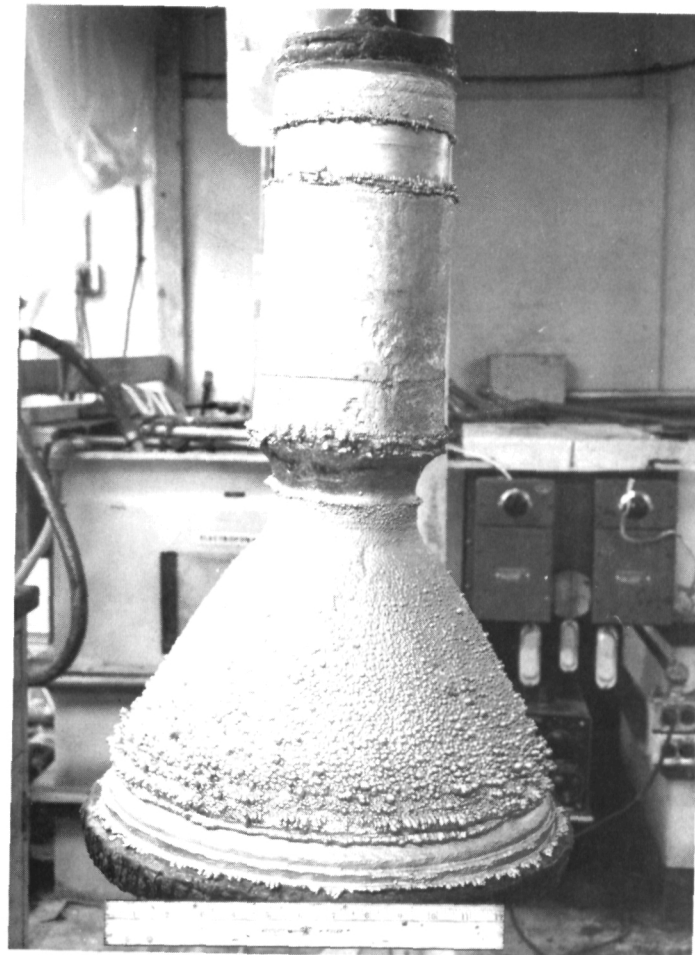
Figure 32. - Thrust chamber at completion of electroforming

Figure 33. - Regeneratively cooled TD nickel-lined thrust chamber.
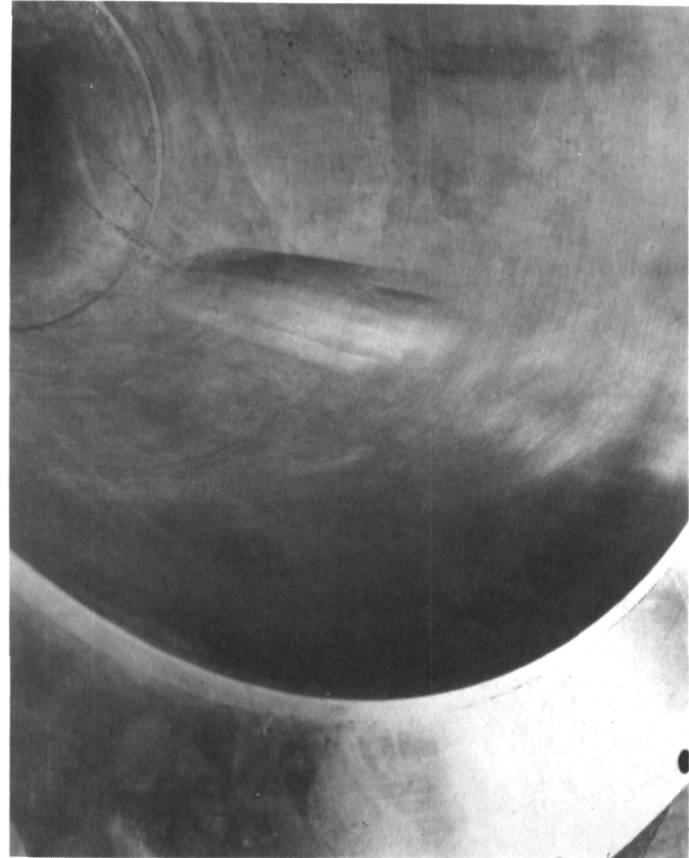
Figure 34. - First liner bulge in nozzle region of thrust chamber.
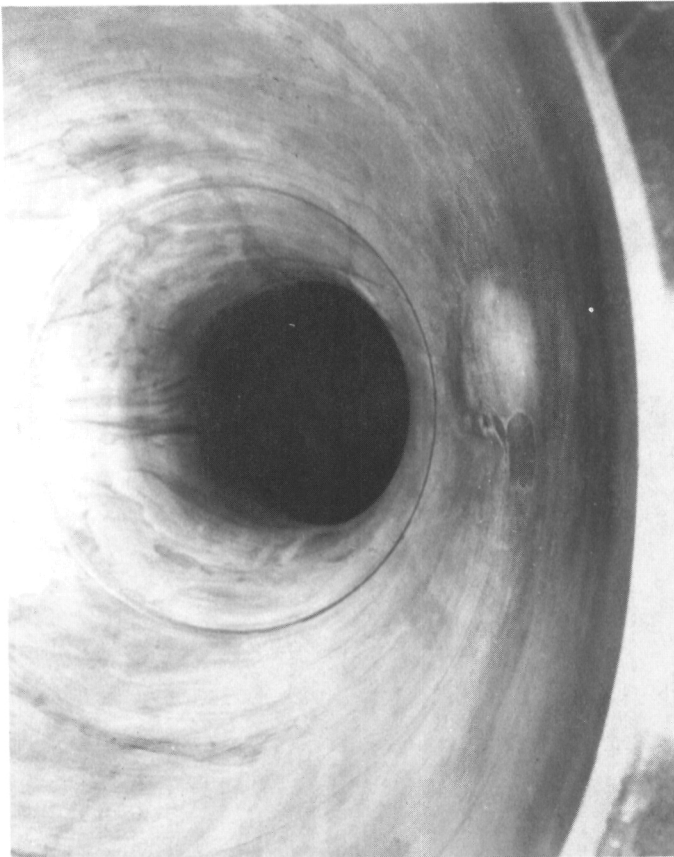
Figure 35. - Second liner bulge in nozzle region of thrust chamber.
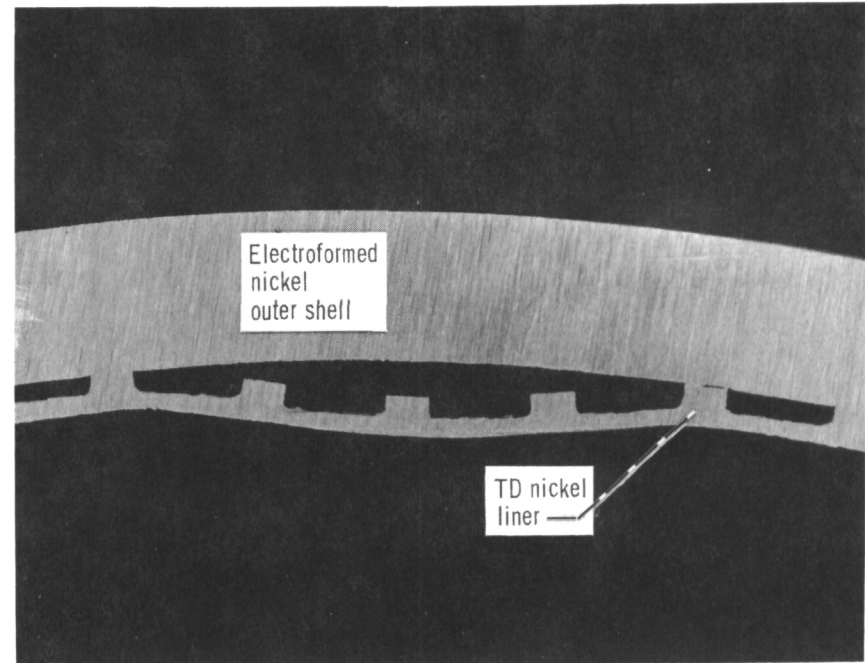
Figure 36. - Section of second bulge area.
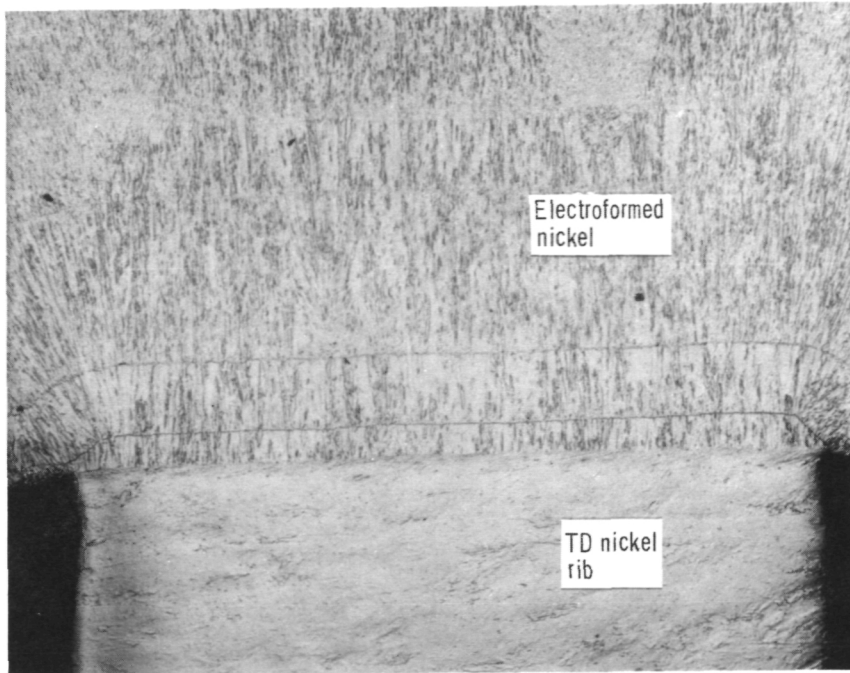
(a) Good electroformed nickel to TD nickel bond adjacent to failure region.
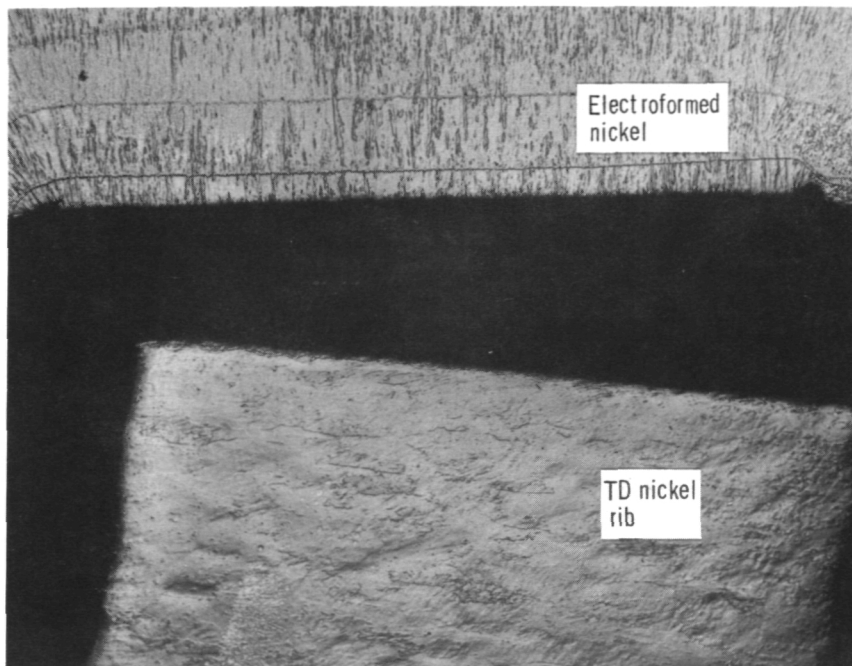
(b) Separated bond in failure region.

Figure 37. - TD nickel rib to outer shell bonds.
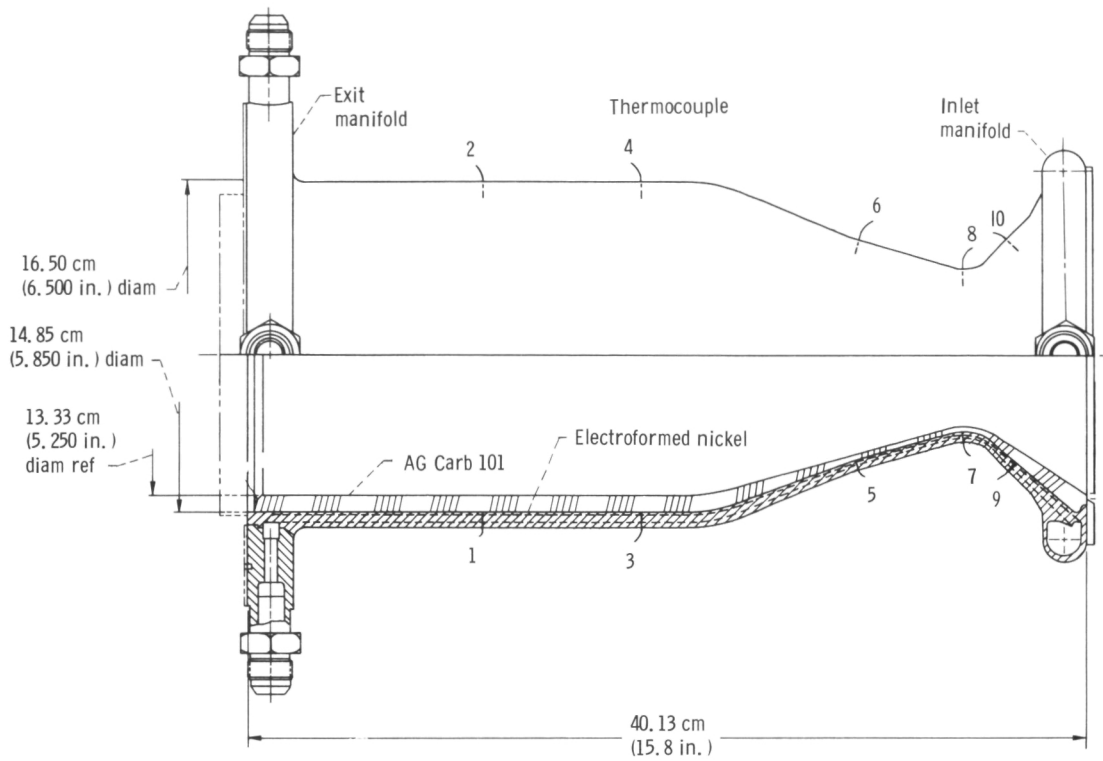
Figure 38. – Graphite-lined thrust chamber design.
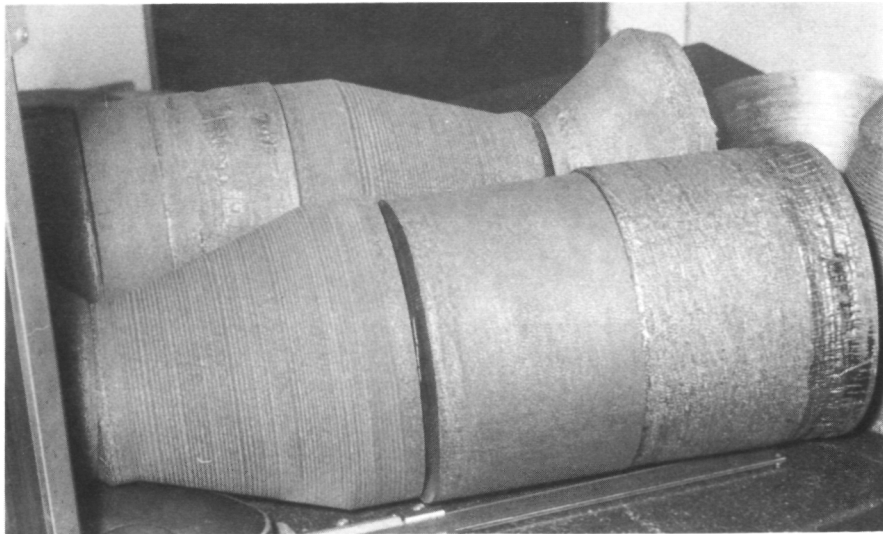
Figure 39. – Four graphite sections for the two chambers assembled before gluing together.

45

Figure 40. - Graphite sections after gluing and machining and before electro-
forming.
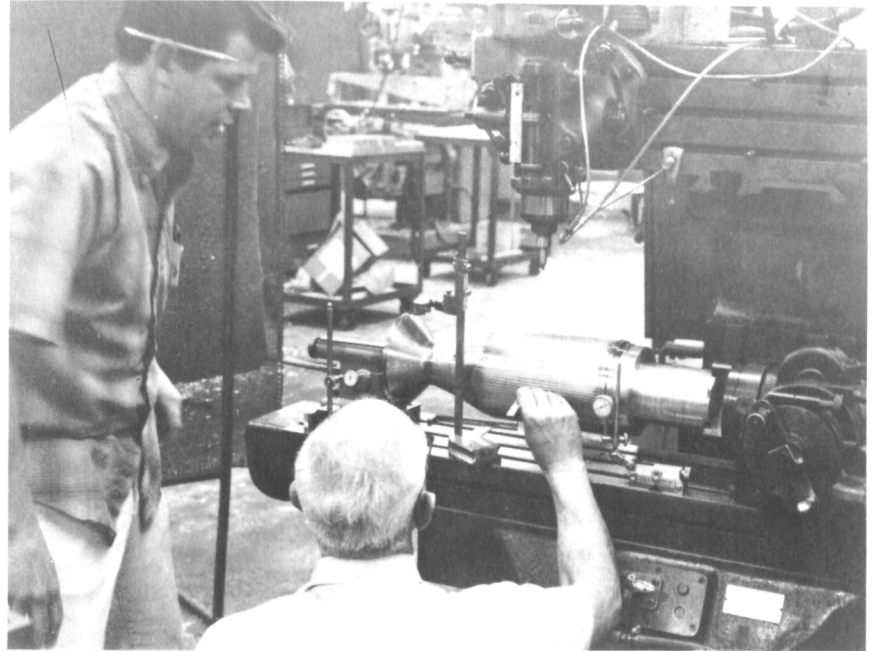
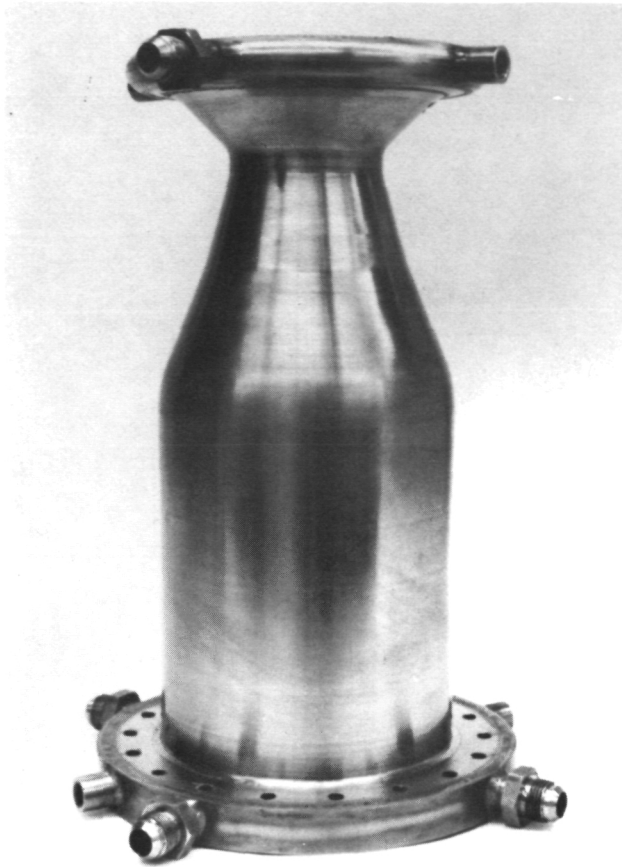Figure 41. - First layer of electroformed nickel with coolant channels being milled.
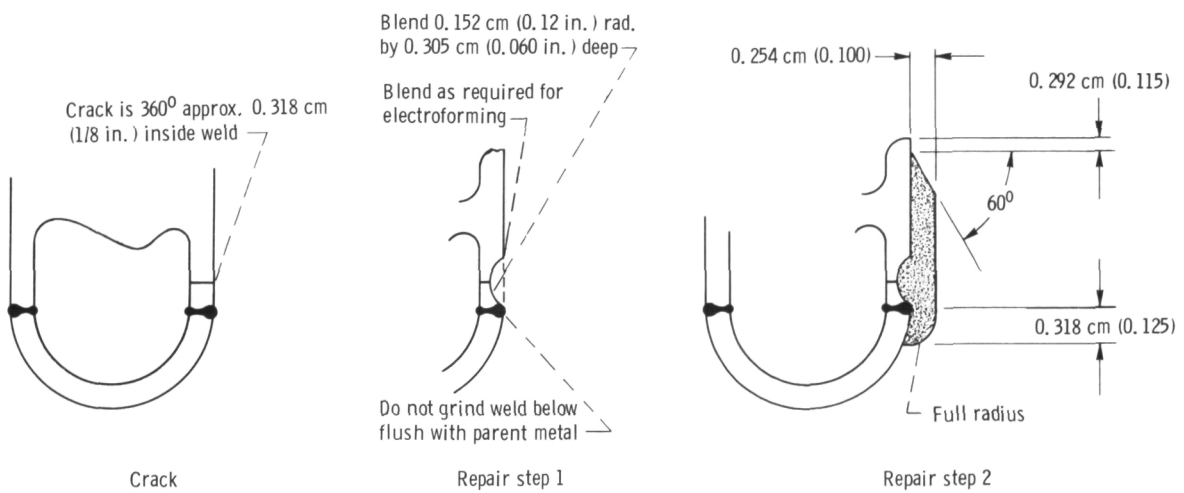
Figure 42. - Completed graphite-lined thrust chamber.

Crack is 360° approx. 0.318 cm (1/8 in.) inside weld

Blend 0.152 cm (0.12 in.) rad. by 0.305 cm (0.060 in.) deep

Blend as required for electroforming

Do not grind weld below flush with parent metal

0.254 cm (0.100)

0.292 cm (0.115)

60°
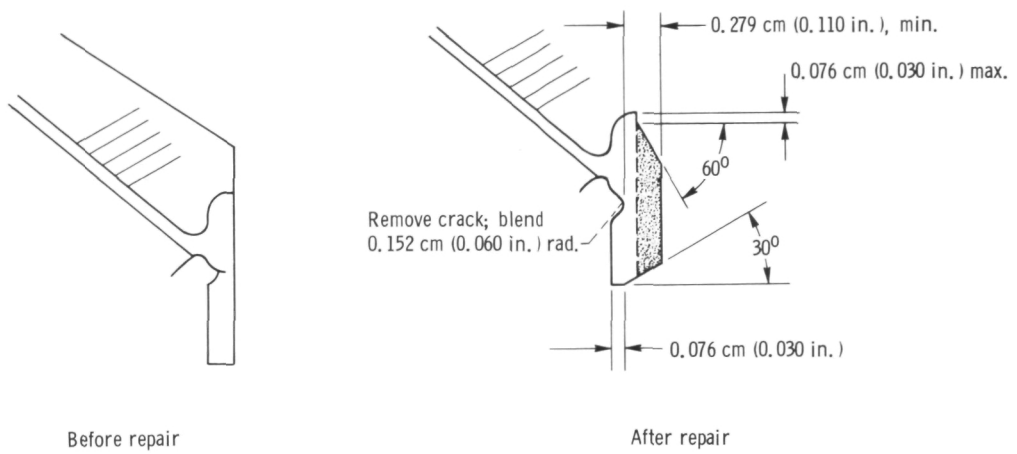
0.318 cm (0.125)

Full radius

Crack

Repair step 1

Repair step 2

Figure 43. - Electroform repair; aft flange serial number 1 thrust chamber. (No scale.)

0.279 cm (0.110 in.), min.

0.076 cm (0.030 in.) max.

60°

Remove crack; blend
0.152 cm (0.060 in.) rad.

30°

0.076 cm (0.030 in.)

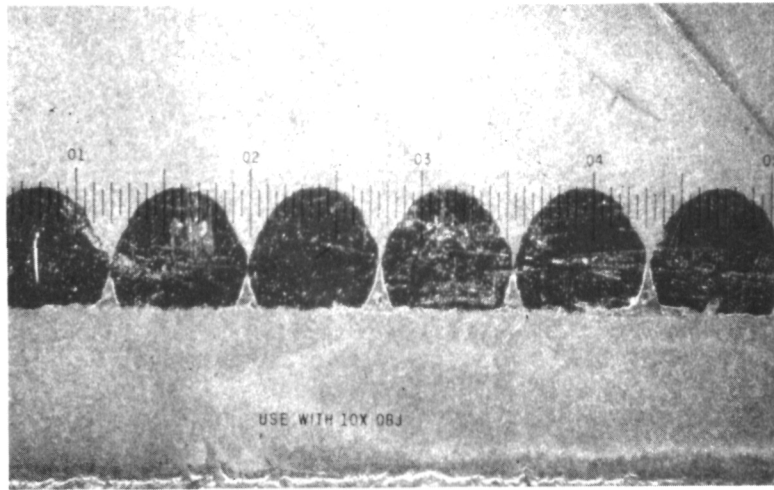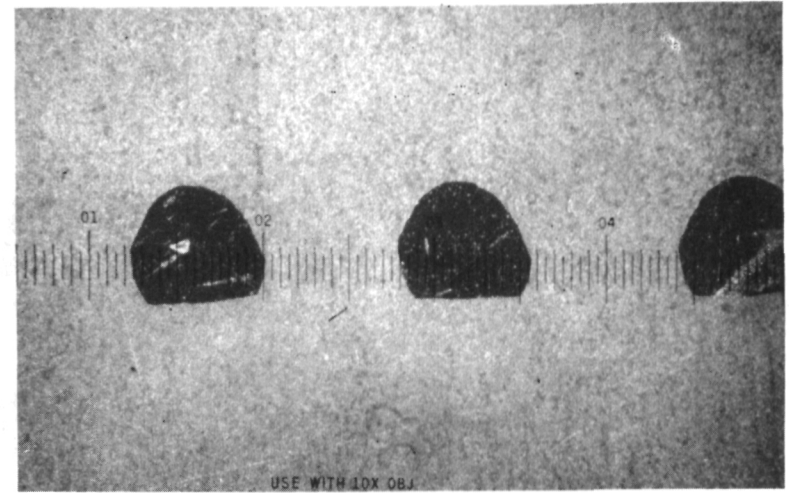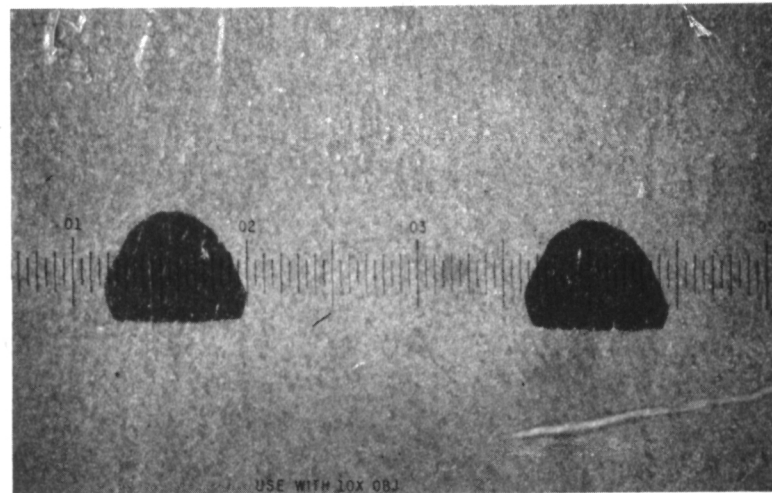Before repair   After repair

Figure 44. – Electroform repair; aft flange serial number 2 thrust chamber.   (No scale.)

48

(a) Wire spacing, nominal.

(b) Wire spacing, 1 diameter.

(c) Wire spacing, 2 diameters.

Figure 45. - Reinforcement of stainless - steel wire in electroformed nickel showing fill with 0.02-cm (8-mil) shaped wire. X100.
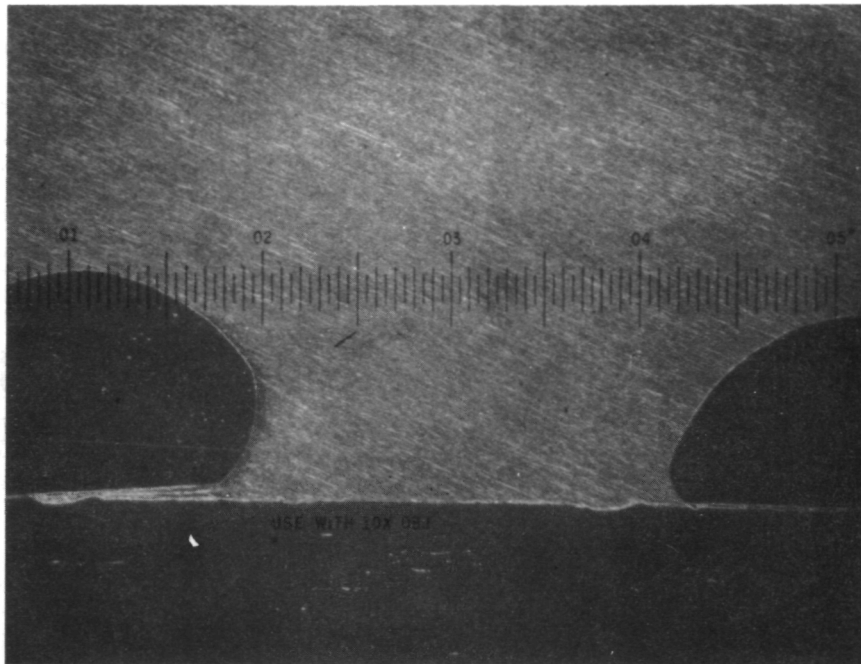
Figure 46. - Reinforcement of stainless-steel wire in electroformed nickel showing fill with 0.05-centimeter (20-mil) shaped wire at one diameter spacing. X100.